Regulation and functional consequences of MCP-1 expression in a model of Charcot-Marie-Tooth 1B disease

Dissertation zur Erlangung des
naturwissenschaftlichen Doktorgrades
der Julius-Maximilians-Universität Würzburg

vorgelegt von
Stefan Martin Fischer
aus Bamberg

Würzburg, 2008

Eingereicht am: _____

Mitglieder der Promotionskommission:
Vorsitzender: Prof. Dr. M. Müller
Gutachter: Prof. Dr. Rudolf Martini
Gutachter: Prof. Dr. Erich Buchner

Tag des Promotionskolloquium:_____
Doktorurkunde ausgehändigt:_____

Für meine Mutter und meine Großmutter

Alltag ist nur durch Wunder erträglich.
Max Frisch (1911-91)

Content:

1. Summary:

Charcot-Marie-Tooth 1B (CMT1B) is a progressive inherited demyelinating disease of human peripheral nervous system leading to sensory and/or motor function disability and is caused by mutations in the P0 gene. Mice heterozygously deficient for P0 (P0+/-) are an adequate model of this human disorder showing myelin degeneration, formation of onion bulbs, remyelination and a reduced motor conduction velocity of around 30m/s similar to patients. Previously, it had been shown that T-lymphocytes and macrophages play a crucial role during pathogenesis in peripheral nerves of P0+/- mice. Both, T-lymphocytes and macrophages increase in number in the endoneurium and deletion of T-lymphocytes or deletion of a macrophage-directed cytokine ameliorates the disease.

In this study the monocyte chemoattractant protein-1 (MCP-1) was identified as an early regulated cytokine before onset of disease is visible at the age of six months. MCP-1 mRNA and protein expression could be detected in femoral quadriceps and sciatic nerves of P0+/- mice already at the age of one month but not in cutaneous saphenous nerves which are never affected by the disease. MCP-1 was shown to be expressed by Schwann cells and to mediate the immigration of immune cells into peripheral nerves. Deletion of MCP-1 in P0+/- mice accomplished by crossbreeding P0 and MCP-1 deficient mice revealed a substantial reduction of immune cells in peripheral nerves of P0+/-/MCP-1+/- and P0+/-/MCP-1-/- mice at the age of six months. In twelve months old mice reduction of immune cells in peripheral nerves is accompanied by amelioration of demyelinating disease in P0+/-/MCP-1+/- and aggravation of demyelinating disease in lumbar ventral roots of P0+/-/MCP-1-/- mice in comparison to P0+/-/MCP-1+/+ mice.

Furthermore, activation of the MEK1/2-ERK1/2 signalling cascade could be demonstrated to take place in Schwann cells of affected peripheral nerves of P0+/- mice overlapping temporarily and spatially with MCP-1 expression. An animal experiment using a MEK1/2-inhibitor *in vivo*, CI-1040, revealed that upon reduction of ERK1/2 phosphorylation MCP-1 mRNA expression is diminished suggesting that the activation of the MEK1/2-ERK1/2 signalling cascade is necessary for MCP-1 expression. Additionally, peripheral nerves of P0+/- mice showing reduced ERK1/2 phosphorylation and MCP-1 mRNA expression also show reduced numbers of macrophages in the endoneurium. This study shows a molecular link between a Schwann cell based mutation and immune cell function. Inhibition of the identified signalling cascade might be a putative target for therapeutic approaches.

2. Zusammenfassung:

Die humane Erkrankung Charcot-Marie-Tooth 1B (CMT1B) ist eine erbliche, chronisch fortschreitende Erkrankung des peripheren Nervensystems die durch Mutation des P0-Gens verursacht wird und zu motorischen und/oder sensorischen Defiziten führt. Sehr ähnlich der humanen Erkrankung weist das Mausmodell, eine für das Myelinprotein P0 heterozygot-defiziente Maus (P0+/-), Degeneration peripheren Myelins, aufeinanderfolgende Zyklen von De- und Remyelinisierung als auch reduzierte Nervenleitgeschwindigkeiten auf. Wissenschaftliche Untersuchungen am Mausmodell ergaben eine Beteiligung von T-Lymphozyten und Makrophagen an der Pathogenese.

In dieser Studie wurde das Chemokin „Monocyte Chemoattractant Protein-1“ (MCP-1) als pathogen-relevant in P0+/- Mäusen identifiziert. MCP-1 mRNA und Protein wurden sowohl im Alter von sechs und zwölf Monaten nachgewiesen, Stadien, in denen morphologische Veränderungen peripherer Nerven von P0+/- Mäusen zu erkennen sind, aber auch im Alter von einen und drei Monaten, ein Alter bei dem pathologischen Veränderungen nicht zu finden sind. Mit Hilfe von MCP-1 defizienten Mäusen (MCP-1-/-) und Verpaarung mit P0-defizienten Mäusen konnten weiterführende Untersuchungen zur Rolle von MCP-1 im peripheren Nerv der Maus durchgeführt werden. So zeigte es sich mittels Transplantation von GFP-positivem Knochenmark, dass MCP-1 die Infiltration von Makrophagen aus dem Blut in periphere Nerven vermittelt. Weiterhin konnte gezeigt werden, dass periphere Nerven von sechs Monate alten P0+/-/MCP-1+/- und P0+/-/MCP-1-/- Mäusen trotz signifikant niedrigerer Anzahl von Immunzellen keine Milderung der Demyelinisierung zeigen. Hingegen weisen periphere Nerven von zwölf Monate alten P0+/-/MCP-1+/- Mäusen sowohl weniger Makrophagen und T-Lymphozyten als auch wesentlich weniger pathologische Veränderungen auf. Periphere Nerven von P0+/-/MCP-1-/- Tieren dagegen zeigen nur eine nicht signifikante Reduktion von Immunzellen und sogar eine Verschlechterung des Phänotyps im Vergleich zu ventralen Spinalwurzeln von P0+/-/MCP-1+/+ Mäusen.

Weiterführende Untersuchungen ergaben, dass eine Aktivierung der MEK1/2-ERK1/2 Signalkaskade sowohl in peripheren Nerven von drei und sechs Monate alten P0+/- Mäusen zu finden ist, allerdings, ähnlich der Expression von MCP-1, nur in peripheren Nerven, die von der Demyelinisierung betroffen sein können. Unter Verwendung eines Inhibitors der Kinasen MEK1 und 2 konnte *in vivo* gezeigt werden, dass Phosphorylierung von ERK1/2 für die erhöhte MCP-1 Expression in peripheren Nerven von P0+/- Mäusen notwendig ist.

Darüber hinaus wurde durch Verminderung der ERK1/2-Phosphorylierung eine Reduktion von Makrophagen im Endoneurium von P0+/- Tieren erzielt.

3. Introduction

The distance between sensory or effector organs in the periphery of a vertebrate organism and the central nervous system is bridged by the peripheral nervous system transmitting informations in a fast and efficient way in both directions. This function of the peripheral nervous system is based on a fine tuned and complex cellular and molecular structure.

3.1 The development of the peripheral nervous system

The neural crest is a cell population derived from and located at the dorsal region of the neural tube which gives rise to a broad spectrum of different cell types like cartilage, smooth muscle, melanocytes but mainly to neurons, enteric glia, satellite cells and Schwann cells (Jessen and Mirsky, 2005). Schwann cells are the major glial cells of the peripheral nervous system migrating as all other cells along specific paths ventral into the mesenchyme of the embryo to reach their point of final destination (Loring and Erickson, 1987; Carpenter and Hollyday, 1992; Sharma et al., 1995).

Main studies to clarify the differentiation of Schwann cells were performed in developing rat sciatic nerves (Jessen et al., 1994; Dong et al., 1995). In rat sciatic nerves of embryonic day 14 to 15 (E14 to E15, similar to mouse E12 to E13) Schwann cell precursors can be found which express low-affinity nerve growth factor receptor p75, the adhesion molecule L1, Cadherin 19 and basal levels of glial cell specific proteins like myelin protein zero (MPZ, P0), peripheral myelin protein 22 (PMP22) and proteolipid protein (PLP) (Jessen and Mirsky, 2005). These Schwann cell precursors are located at the margin and within the prospective nerve, they do not exhibit a basal lamina (Wanner et al., 2006) and their survival is critically dependent on the contact to axons. Neuregulin 1 type III mediates contact-dependent survival of Schwann cell precursors (Dong et al., 1995; Riethmacher et al., 1997; Morris et al., 1999; Woldeyesus et al., 1999) and additionally the migration beyond the location of dorsal root ganglions (Britsch et al., 1998).

Around two to three days later in development, at E17, when endoneurial connective tissue, vascularisation and the first cell layer of perineurium occur, the majority of Schwann cells in rats exhibit a basal lamina, express octamer-binding transcription factor 6 (OCT6), S100β calcium-binding protein (S100β) and glial fibrillary acidic protein (GFAP) and, most

importantly, survive because of autocrine secretion of Insulin-like growth factor 2 (IGF2), neurotrophin 3 (NT3), platelet-derived growth factor-β (PDGF-β) and leukaemia inhibitory factor (LIF, Meier et al., 1999; Jessen and Mirsky, 2005). These so called immature Schwann cells collectively ensheath large numbers of axons, by that forming Schwann cell families.

At this stage a process called radial sorting takes place which is a prerequisite for the formation of adult nerve fibers (Jessen and Mirsky, 2005). In this process large diameter axons, also defined as myelin-competent axons, are sorted out of the Schwann cell families leading to a 1:1 ratio between axons and Schwann cells. This process is inhibited in mice carrying either a conditional knock out for β1 integrin (Feltri et al., 2002) or a gene deletion for the gene encoding for laminin α4 (Wallquist et al., 2005). Furthermore, inhibition or genetically deletion of the Rho GTPases cdc42 or rac1 results in an impaired radial sorting (Benninger et al., 2007; Nodari et al., 2007). In the following, Schwann cells associated with myelin-competent axons start to form myelin sheaths at around E20 which continues postnatally whereas small diameter axons remain ensheathed in groups by non-myelinating Schwann cells.

3.2 The structure of myelin sheaths

The myelin sheath is formed by Schwann cells wrapping several times around the associated axon. After some turns of a Schwann cell process apposing membranes of myelin spirals are compressed. For this purpose the cytoplasm is squeezed out and the formation is stabilised by myelin proteins (Martini, 2004).

One Schwann cell myelinates only a segment of up to 1.5 mm along one axon leading to coverage of axons by consecutive Schwann cells forming myelin sheaths. The region along the axons covered mainly by compact myelin of Schwann cells, called the internode, serves as a lipid based electric insulator accelerating the conduction of action potentials along a nerve fiber. Between consecutive Schwann cells non-myelinated regions termed nodes of Ranvier enable the exchange of ions between axoplasm and extracellular space leading to a saltatory way of action potential transmission. The saltatory nerve conduction is a rapid and energy-saving mechanism which enables also small nerve fibers to effectively propagate action potentials. The structure of the nodes of Ranvier is composed of a nodal, paranodal and juxtaparanodal region which, due to their distinct molecular composition, form the basement for saltatory nerve conduction (Poliak and Peles, 2003).

Due to the large area covered by Schwann cells, the big membrane compartment and complex supportive functions for axons myelin sheaths exhibit additionally to the nodes of Ranvier two more functional compartments, the compacted and non-compacted myelin. Both compartments have distinct molecular composition. Compact myelin harbours P0 (~50% of total protein, Niemann et al., 2006). P0 is the most abundant and most important myelin protein in peripheral nerves. It belongs to the immunoglobulin superfamily and consists of an extracellular Ig-domain, a transmembrane and a basic intracellular domain. The extracellular domain interacts homophilically in cis and trans forming the intraperiod line, whereas the intracellular domain is thought to interact with negatively charged phospholipids of the adjacent intracellular Schwann cell membrane leaflet forming the major dense line (Trapp, 2004). In addition it was shown *in vitro* that in the intracellular part of P0 a protein kinase C alpha (PKCα) substrate motif exists and, furthermore, the activity of PKCα is important for adhesive function of P0 (Xu et al., 2001; Gaboreanu et al., 2007). Another myelin protein in compact myelin is peripheral myelin protein 22 (PMP22, 2-5% of total protein, Niemann et al., 2006). Compact myelin functions mainly as electric insulator and structural scaffold.

Uncompacted myelin as periaxonal collars, paranodal loops and Schmidt-Lanterman incisures are regions where Schwann cell cytoplasm can be found. Typical proteins at these sites are myelin associated glycoprotein (MAG, Trapp, 2004), which has a function in signalling events in Schwann cells and possibly also during initial events of myelination, and Gap junction tunnel proteins, like e.g. Connexin32 (Cx32). Gap junctions in uncompacted regions of myelin sheaths are thought to have a critical function in transporting metabolites, proteins and signals between Schwann cell body and adaxonal regions (Paul, 1995). Genes encoding for myelin-related proteins like P0, PMP22 and gap junction proteins are of particular interest for this study due to their role in inherited peripheral neuropathies.

3.3 Inherited peripheral neuropathies

Charcot-Marie-Tooth (CMT) diseases, also called hereditary motor and sensory neuropathies form a major group of human disorders in the peripheral nervous system with high incidence (4 patients out of 10 000 individuals, Skre, 1974) leading to chronic and progressive degeneration of peripheral nerves. Jean Martin Charcot and Pierre Marie in France and Howard Henry Tooth in England described first at the end of the 19th century clinical cases of familiar inherited disorders starting with weakness followed by muscle atrophy of lower and eventually later on of upper extremities.

Nowadays it is known that mutations in several different genes cause a variety of different but similar CMT diseases. In general, CMT cases are classified in four different groups, namely CMT1, CMT2, CMTX and CMT4 which are subdivided based on the mutation of a certain glial- or neuronal-related gene (Shy et al., 2002). Mutated genes involved are coding for proteins of different functions like P0, PMP22, Cx32, Periaxin and proteolipid protein as components of myelin. Beside that mutations in the transcription factors Krox20 and Sox10 altering the transcription of important myelin proteins and mutations in proteins belonging to the endocytosis, sorting or degradation apparatus like Dynamin 2, Rab7 or SIMPLE were shown to cause CMT (Niemann et al., 2006).

Cases of peripheral neuropathies which are recessively inherited are designated CMT4 and occur very rarely. Most cases of CMT4 are severe neuropathies with onset before birth or during infancy (Suter and Scherer, 2003). In 10-15% of CMT-patients the disease is dominantly X-linked inherited and is called CMT1X. CMT1X is caused by more than 240 different mutations in the gene *GjB1* encoding for Cx32 or the corresponding promoter region. Therefore, a wide variety of weakness, muscle atrophy and sensory loss is known as clinical phenotype. Many CMT1X patients exhibit normal nerve conduction velocities but very decreased amplitudes suggesting axonal loss which could be confirmed by sural nerve biopsies (Hahn et al., 1990; Shy et al., 2002).

CMT2 is dominantly inherited and onset of disease varies between 10 years of age up to older than 30 years. The nerve conduction velocities of patients suffering from CMT2 are normal but evoked compound motor and sensory amplitudes are reduced indicating loss of axons in peripheral nerves (Suter and Scherer, 2003).

CMT1, which is the type of disease discussed in this work, is a primarily demyelinating disease which can be diagnosed electrophysiologically by a reduction of nerve conduction velocities (< 38 m/s). Symmetrical muscle weakness, muscle atrophy and sensory loss are typical clinical features. Demyelination occurs segmentally and is paralleled by remyelination (Suter and Scherer, 2003) characterized by thinner myelin sheaths and shorter internodes as before demyelination (Blakemore, 1974; Ludwin and Maitland, 1984).

In human peripheral neuropathies like CMT1 demyelination and remyelination occur periodically and leads after several rounds to the appearance of onion bulbs. Onion bulbs are formed by supernumary Schwann cells building up concentric cell layers around thin and demyelinated axons (Naba et al., 2000). These Schwann cells show an expression pattern similar to immature Schwann cells (Guenard et al, 1996) which leads to the conclusion that

Schwann cells of demyelinating peripheral nerves undergo a dedifferentiation program to start remyelination again (Harrisingh and Lloyd, 2004).

More than 50% of CMT1 patients carry a duplication of 1.5 mega base pairs containing the gene encoding PMP22 on chromosome 17 leading to CMT1A with a typical disease onset during first decade of life (Suter and Snipes, 1995). Rats and mice carrying extra transgenic copies of PMP22 also develop a similar neuropathy like humans and are used as animal models (Huxley et al., 1996; Sereda et al., 1996; Martini, 1997; Huxley et al., 1998). In addition, point mutations with low incidence in PMP22 in humans can lead to a CMT1 or, in more severe cases to another disease called Dejerine-Sottas syndrome (DSS) with onset during early neonatal period. Furthermore, heterozygous deletion or reduction of PMP22-expression develops in humans an asymmetrical demyelinating disorder with transient weakness and sensory loss named hereditary neuropathy with liability to pressure pulsies (HNPP, Shy et al., 2002; Suter and Scherer, 2003).

Point mutations in the most abundant myelin protein P0 also can cause DSS and CMT disorder namely CMT1B, clinically similar to CMT1A. Point mutations in the gene encoding for P0 and leading to inherited peripheral neuropathies are situated in the extracellular, transmembrane or intracellular domain of P0 suggesting that each part of the protein has essential properties for protein function (Shy et al., 2002; Shy, 2006).

3.4 P0 heterozygously deficient mice as model for CMT1B

Mice heterozygously deficient for P0 (P0+/-) are an adequate animal model for human CMT1B disease (Martini, 1997). Peripheral nerves of P0+/- mice show normal development until the age of 10 weeks but progressive demyelinating disease is evident after the age of four months (Martini et al., 1995a). Peripheral nerves of P0+/- mice exhibit myelin degeneration, formation of onion bulbs, remyelination and a reduced motor conduction velocity of around 30m/s similar to patients.

Previous studies showed a clear impact of the immune system on the progression of inherited peripheral neuropathy in these mice. In 2000 Christoph Schmid and colleagues reported about first evidences of a crucial influence of the immune system in P0+/- mice (Schmid et al., 2000). During aging the cell numbers of CD8+ T-lymphocytes and macrophages elevate in the endoneurium of femoral quadriceps nerves in P0+/- mice compared to P0+/+ mice.

To further elucidate the putative function of these cells, P0+/- mice carrying in addition an immune deficiency were generated by crossbreeding with recombination activating gene-1 (RAG-1) deficient mice. A non functional RAG-1 gene leads to the absence of mature B- and T-lymphocytes (Mombaerts et al., 1992). The absence of key players of adaptive immunity results in a lower g-ratio, which is an indicator for thicker myelin sheaths, and better nerve conduction velocities in P0+/- mice. Interestingly, the absence of T-lymphocytes also leads to a reduced occurrence of macrophages in quadriceps nerve. Another immune deficiency in P0+/- mice namely deficiency in T-cell receptor α (TCRα) also reduces pathological profiles (Schmid et al., 2000).

Macrophages are very important in the peripheral nervous system especially after injury. After injury high numbers of macrophages which phagocytose myelin debris, modulate the extracellular matrix and thereby clear inhibitory factors for axonal regrowths are recruited to injured nerves. This allows a better and more efficient regeneration of peripheral nerves in contrast to injuries in the central nervous system (Stoll et al., 2002; Vargas and Barres, 2007).

To elucidate the role of macrophages in animal models of inherited peripheral neuropathies the P0+/- mice were crossbred with osteopetrotic mice (Carenini et al., 2001). Osteopetrotic mice carry a mutation in *csf1* leading to a deficiency of macrophage colony stimulating factor (M-CSF, Yoshida et al., 1990). Stefano Carenini and colleagues showed in 2001 that peripheral nerves of M-CSF deficient P0+/- mice exhibit reduced numbers of macrophages and lower g-ratios than P0+/- mice without deficiency for M-CSF. In addition, deficiency of M-CSF yields slightly lower cell numbers of CD8+ T-lymphocytes in peripheral nerves suggesting a direct or indirect interaction between macrophages and T-lymphocytes.

Already in the year 1993 Vass and colleagues recognized that in peripheral nerves of rats macrophages undergo a turn-over (Vass et al., 1993). This observation has been successfully confirmed by Mathias Mäurer and colleagues in the year 2003 in P0+/+ and P0+/- mice (Maurer et al., 2003). For this approach bone marrow from transgenic mice carrying an ubiquitously expressed GFP-transgene was transplanted into lethally irradiated P0+/+ and P0+/- mice and analyzed four months later. This study showed that after four months 60% of endoneurial macrophages express GFP, which means they had recently immigrated into peripheral nerves. Additionally, it was found by using immunohistochemistry that long-term resident macrophages (GFP-) and short-term endoneurial macrophages (GFP+) carry myelin basic protein reactive structures suggesting that both types of macrophages are involved in myelin destruction in P0+/- mice.

In 2007 Dr. Marcus Müller and colleagues investigated whether M-CSF is an important factor for activation and expansion of long-term resident, GFP-negative and/or recently immigrated, GFP-positive macrophages in the endoneurium of P0+/- mice (Muller et al., 2007). Therefore, GFP+ bone marrow chimeras of P0+/-/M-CSF-competent and P0+/-/M-CSF-deficient mice were analyzed. It could be shown that M-CSF is acting on both types of macrophages, GFP+ and GFP-. The ratio of GFP+ versus GFP- macrophages was similar in peripheral nerves of P0+/-/M-CSF-competent and P0+/-/M-CSF-deficient mice whereas the total number was significantly decreased in P0+/-/M-CSF-deficient mice. Therefore, M-CSF was identified as crucial cytokine for the GFP+ and GFP- macrophages in peripheral nerves.

Another important cytokine targeting macrophages is the monocyte chemoattractant protein-1 (MCP-1), also known as (C-C motif) ligand 2 (CCL2). MCP-1 is a CC chemokine and exhibits chemoattractive function to macrophages, natural killer cells and T-lymphocytes (Lu et al., 1998). In experimental autoimmune encephalomyelitis (EAE), an animal model for multiple sclerosis, deficiency of MCP-1 leads to a reduced macrophage recruitment and inflammation (Huang et al., 2001).

3.5 Aim of the study

Inherited peripheral neuropathies are chronic progressive demyelinating disorders. Charcot-Marie-Tooth 1 (CMT1) diseases are a genetically heterogeneous group of demyelinating disorders of the peripheral nervous system.

In mouse models of CMT1B, mice heterozygously deficient for P0 (P0+/-), it could be shown previously that macrophages play a central role in mediating the demyelination. Therefore, we examined the contribution of monocyte chemoattractant protein-1, MCP-1 as an important cytokine for macrophage migration and activity to the progression and outcome of an inherited neuropathy in peripheral nerves of P0+/- mice in comparison to P0+/+ mice. Furthermore, signal transduction pathways possibly involved in the induction of MCP-1 expression in the mutants were examined to identify molecular targets for putative therapeutic approaches.

4. Materials and methods

4.1 Equipment, media, buffers, solutions, reagents and chemicals

Detailed information about technical equipment (Appendix 7.1), media and other solutions for cell culture experiments (Appendix 7.2), buffers (Appendix 7.3), primer sequences (Appendix 7.4), target sequences for *in-situ* hybridisation (Appendix 7.5), as well as antibodies used for western blot analyses (Appendix 7.6) and immunohistochemistry (Appendix 7.7) is provided in the Appendices.

4.2 Animal husbandry

Mice heterozygously deficient for P0 (P0+/-, Giese et al., 1992) were backcrossed for more than 20 generations to a C57/B6 background. Mice homozygously deficient for MCP-1 with 129Sv/J and C57/B6 mixed background (MCP-1-/-, Lu et al., 1998) were provided by Dr. Barret Jon Rollins, Harvard Medical School, USA. GFP transgenic mice (Okabe et al., 1997) were kindly provided by Dr. Reinhard Kiefer, Department of Neurology, Westfälische Wilhelms-Universität, Münster, Germany. P0 and MCP-1 deficient mice were crossbred following previously published protocols (Schmid et al., 2000; Carenini et al., 2001). Littermates were analysed in each experiment.

All mouse strains used in this study were kept under barrier conditions at the Department of Neurology, Julius-Maximilians-Universität, Würzburg, Germany. Animal experiments were approved by the local authorities (Regierung von Unterfranken).

4.3 Phenotyping of GFP-transgenic mice and genotyping of P0 and MCP-1 gene knockout mutation by polymerase chain reaction

GFP-transgenic mice were bled from the tail vein and blood smears were analysed for GFP+ leukocytes using a fluorescence microscope.

Genotyping of P0 and MCP-1 deficient mice was performed by polymerase chain reaction (PCR) amplifying the wild type allele, P0 or MCP-1, respectively, and the neo resistance cassette which was introduced at the site of the knocked-out wild type gene. Genomic DNA was purified from tail biopsies using DNeasy blood & tissue kit from Qiagen (Hilden, Germany) according to the guidelines of manufacturer.

The PCR reaction for amplification of the P0 wild type gene (Schmid et al., 2000) consists of 0.5 U taq polymerase (Applied Biosystems, Foster City, CA 94404, USA), 0.2 µM dNTP, 1.5 mM $MgCl_2$, 0.25 µM *primer S* 1295 and 0.25 mM primer *AS 1772* (for primer sequences see Appendix 7.4). The knock-out allele was amplified using the same reaction conditions except using 0.25 mM primer *AS 1606* instead of primer *AS 1772*. For both PCR reactions an annealing temperature of 55°C was used.

The PCR reaction for amplification of the MCP-1 wild type gene (Lu et al., 1998) consists of 1.5 U taq polymerase (Applied Biosystems, Foster City, CA 94404, USA), 0.4 µM dNTP, 3 mM $MgCl_2$, 0.2 µM *MCP-1 F primer* and 0.2 µM *MCP-1 R primer*. The corresponding knock-out allele was amplified using the same reaction conditions except using 0.25 µM *IMRO 60 primer* instead of *MCP-1 R primer*. The annealling temperature for both reactions was 59°C.

All primers were synthesized by Sigma Genosys (Taufkirchen, Germany). PCR products were analysed in 1% or 2% agarose gels in TBE buffer (89 mM Borate, 89 mM Tris(hydroxymethyl)aminomethane acetate, 2 mM EDTA, pH 8.0) stained with ethidiumbromide.

4.4 Total RNA and protein isolation by acidic guanidinium thiocyanate-phenol-chloroform extraction

Total RNA was isolated by acidic guanidinium thiocyanate-phenol-chloroform extraction (Chomczynski and Sacchi, 1987) from sciatic nerves, femoral quadriceps and cutaneous saphenous nerves, lumbar ventral and dorsal roots of single mice using TRIzol® reagent from Invitrogen (Karlsruhe, Germany). Mice were deeply anesthetized, peripheral nerves were quickly dissected and immediately freezed in liquid nitrogen. Homogenization of peripheral nerves in TRIzol® was performed using an ultrathurax from ART Labortechnik

(Mühlheim, Germany). Total RNA and proteins were isolated by Phenol-Chloroform extraction, phase separation and subsequent precipitation accordingly to the instructions of manufacturer.

RNA Pellets were solubilized in DEPC-water and RNA concentrations were measured using a photometer (Eppendorf, Hamburg, Germany). RNA samples showing a 260nm/280nm ratio less than 1.70 were either neglected or subsequentialy Phenol-Chloroform extracted again and precipitated with isopropanol (Joseph Sambrook, 2001).

Protein pellets were achieved by precipitation of phenolic phase with isopropanol. Protein pellets were washed three times with 0.3M guanidine hydrochloride in 95% ethanol, one time with ethanol for twenty minutes each and dried for a few minutes using a speed vac (UniEquip, Planegg, Germany). Subsequentially proteins were solubilized in 1% SDS. Concentration of resulting protein samples were examined by a Lowry assay (Lowry et al., 1951, Sigma Aldrich, Taufkirchen, Germany) using bovine serum albumine (BSA) in SDS as standard.

4.5 cDNA synthesis and semiquantitative real-time PCR

Total RNA (0.5 or 1 µg) was transcribed into cDNA using TaqMan Reverse Transcription Reagents accordingly to the instruction of manufacturers (Applied Biosystems, Foster City, CA 94404, USA). The resulting cDNA was used for TaqMan assays for semiquantitative real-time PCR (qRT-PCR).

qRT-PCR was performed using pre-developed TaqMan assays (Murine MCP1, 4329581F; Mouse M-CSF, Mm00432688_m1; Eukaryotic 18S rRNA Endogenous Control, 4319413E; Murine TNFα, Mm00443258_m1; IL-10, Mm00439616_m1; IL-6, Mm00446190_m1; IFNγ, Mm00801778_m1, GM-CSF, Mm00438328_m1; IL-1β, Mm00434228_m1) and TaqMan universal PCR master mix (Applied Biosystems, Foster City, CA 94404, USA) according to the manufacturers´ guidelines. All samples were measured in triplicates. Data sets were analysed in relation to 18s RNA content and were related to samples of wild type nerves.

4.6 Detection of MCP-1 and M-CSF by enzyme-linked immunosorbent assay

Peripheral nerves (sciatic, femoral quadriceps and cutaneous saphenous nerves) from P0+/+/MCP-1+/+, P0 +/-/MCP-1+/+ at the age of 1 month (n = 5 / 5), 3 months (n = 5 / 5), 6 months (n = 3 / 5) and from 6 months old P0+/-/MCP-1+/- (n = 5) and P0+/-/MCP-1-/- (n = 3) mice were dissected, frozen in liquid nitrogen and sonicated in a volume of 100 µl RIPA lysis buffer per 10 mg tissue.

After determination of protein concentration by a Lowry assay (Lowry et al., 1951, Sigma Aldrich, Taufkirchen, Germany) lysates were used to quantify the amount of MCP-1 and M-CSF protein per total protein by using the corresponding Quantikine ELISA kit (R&D systems, Minneapolis, MN 55413, USA). In addition, MCP-1 protein in cell culture supernatants and cell lysates from Rn22 cells was also measured by MCP-1 Quantikine ELISA kit (R&D systems, Minneapolis, MN 55413, USA).

4.7 Western blot analysis

Western blot analyses were performed on protein lysates from sciatic, femoral quadriceps and cutaneous saphenous nerves from single mice to quantify phosphorylated and unphosphorylated kinases. Mice were deeply anesthetized and perfused transcardial with PBS (phosphate buffered saline) for up to two minutes to minimise contamination with blood during preparation. At the beginning of the experiments some mice were sacrificed to examine if a short perfusion had an impact on the activation of signalling cascades in peripheral nerves. Nerves which were immediately dissected after death and nerves which were prepared later showed no obvious differences. After quick dissection of peripheral nerves the tissue were immediately freezed in liquid nitrogen and stored on maximal –80°C. During the dissection extreme caution was always taken not to harm the peripheral nerves before the nerve was transected (Doya et al., 2005). Corresponding to the weight of the tissue RIPA lysis buffer were added (100 µl/10 mg tissue) and the tissue was homogenized by sonication two times for 30 seconds on ice (Sonoplus HD60, Bandelin electronic, Berlin, Germany). Following centrifugation for one minute at 4.000 xg the amount of total proteins in the clarified supernatants was analysed by a Lowry assay (Sigma, Taufkirchen, Germany,

Lowry et al., 1951). BSA in different concentrations solved in RIPA buffer was used as standard.

Equal amounts of proteins were taken for Western blot analyses. Samples were mixed 3:1 with Roti® Load 1 buffer (Carl Roth, Karlsruhe, Germany), denatured for three minutes at 95°C and added into a polyacrylamide gel (SDS-PAGE). The SDS-PAGE was performed according to Laemmli (Laemmli, 1970). Gels were produced in the lab and were run on a Bio-Rad Mini-Protean® 3 electrophoresis module (Bio-Rad Laboratories, München, Germany). After SDS-PAGE proteins were transferred on nitrocellulose membranes (Schleicher & Schuell BioScience, Keene, NH 03431, USA) using a Bio-Rad Mini Trans-Blot® module (Bio-Rad Laboratories GmbH, München, Germany) at 400 mA with an ice-cooling unit inside. Subsequently, the nitrocellulose membranes were stained with Ponceau S (0.1% (w/v) Ponceau S in 1% (w/v) Trichloracetic acid) and the resulting staining was documented.

Detection of distinct proteins was performed by using specific antibodies (see appendix 7.6). Firstly, the membrane was blocked for at least 30 minutes at room temperature with either milk powder (5 % in PBST) or BSA (5 % in PBST) depending on the primary antibody used. Secondly, after washing the membrane with PBST, the primary antibodies diluted in PBST were incubated for two hours at room temperature or over night at 4°C. After washing three times for five minutes with PBST corresponding secondary antibodies were added in PBST for 30, 60 or 120 minutes. Following three wash steps with PBST, the antibody reaction was examined by using ECL substrate reagent according to the guidelines of manufacturers (GE Healthcare, München, Germany). Chemiluminescence was detected on Hyperfilm™ ECL (GE Healthcare, München, Germany) for several time points.

Loading controls were achieved by staining especially the corresponding unphosphorylated kinases on the same membrane after stripping off the antibodies of previous reactions (30 - 120 minutes incubation with stripping buffer at room temperature). Disappearance of previous primary antibody was controlled by immune detection using only secondary antibodies

4.8 Cell culture experiments

Lysates of cultured NIH 3T3 (mouse fibroblast cell line) and HeLa cells (human cervical cancer cell line) were used as controls in western blot analyses. NIH 3T3 and HeLa cells

were cultured in commercially available DMEM (Invitrogen GmbH, Karlsruhe, Germany) substituted with 10 – 20% Foetal calf serum (FCS, Biochrom, Berlin, Germany) and 2 mM glutamine (Invitrogen, Karlsruhe, Germany). Culture splitting was achieved by trypsination of cells (Invitrogen, Karlsruhe, Germany) and 1/10 dilution in new culture dishes.

Some NIH 3T3 cultures of around 80% confluency were cultured in DMEM with 0.05% serum overnight. On the next day 10% FCS was added to some culture dishes and incubated for thirty minutes. Afterwards cells were harvested using cell scraper and lysed in RIPA buffer. Resulting lysates were used for the detection of MAPK- and NFκB- pathway related proteins via immunoblot. In other cases NIH 3T3 and HeLa cells were cultured until 80% confluency and irradiated with 100 J/m^2 (UV Crosslinker 1800, Stratagene, La Jolla, CA 92037; USA). Cells were afterwards harvested as described above and activation status of p38 and JNK kinase were evaluated.

In other experiments the rat Schwannoma cell line Rn22 was used. Rn22 cells were also cultured in DMEM (Invitrogen, Karlsruhe, Germany) substituted with 10% FCS (Biochrom, Berlin, Germany) and 2 mM glutamine (Invitrogen, Karlsruhe, Germany). In some cases LIF or IL-6 (10 ng/ml, Peprotech EC Ltd, London, UK) was added to the medium. Additionally, some Rn22 cultures were treated with or without 10 µM CI-1040 (kindly provided by Pfizer New York, USA) for three hours and subsequentially the cells were harvested (see above).

4.9 Immunohistochemistry

Tissue was taken from PBS perfused mice for the detection of F4/80-, CD8-, CD4- (Carenini et al., 2001) and phosphoERK1/2-positive profiles on cross sections of fresh frozen tissue. For the detection of CD68+ profiles in GFP bone marrow transplanted mice (see section 4.9), animals were perfused for five minutes with PBS and subsequently with 4% paraformaldehyde (PFA) in PBS for 20 minutes. Peripheral nerves were embedded in O.C.T. matrix (DiaTec, Nürnberg, Germany) and cut into 10-µm-thick sections on a cryostat (Leica, Wetzlar, Germany).

The detection of phosphorylated ERK1/2 (phosphoERK1/2) and total ERK1/2 were additionally performed on single fiber preparations. For this purpose mice were transcardially perfused with PBS for five minutes and subsequently with 2% PFA/PBS for 10 minutes. Peripheral nerves were dissected, the epineurium was stripped off and the nerve fibers were teased. Immunohistochemical staining was accomplished free floating. As control for

immunohistochemical stainings against phosphorylated and unphosphorylated ERK1/2 proteins NIH 3T3 cells cultured on cover slides in DMEM with 0.05% FCS and DMEM with 10% FCS was used (see section 4.7).

Detailed informations about distinct stainings are listed in the appendix 7.7. In general, after fixation the specimens were blocked with 5% BSA in PBS for 30 minutes and subsequently incubated with primary antibody (for concentrations see appendix 7.7) over night at 4°C. After washing three times with PBS secondary antibodies were added for 45 to 60 minutes at room temperature. Stainings against F4/80, CD8, and CD4 were finalised using StreptABComplex kit (DakoCytomation, Hamburg, Germany). Substrate reactions were performed using Diaminobenzidine (1 mg/ml) substituted with 0.02% H_2O_2. Colorimetric stainings were embedded in Aquatex (Merck, Darmstadt, Germany) whereas fluorescence stainings were embedded in DABCO (25 ml PBS, 75 ml glycerol, 2.5 g 1,4-diazabicyclo[2.2.2]octane) and kept dark at –20°C. Quantification of macrophages, T-lymphocytes and DAPI-positive nuclei per cross section was performed by investigators being not aware of the genotype on minimal six sections per animal..

4.10 Transplantation of GFP+ bone marrow

At the age of three months, mice were bone marrow transplanted (Okabe et al., 1997; Maurer et al., 2003; Muller et al., 2007). Bone marrow was taken from adult GFP-transgenic mice and $2x10^7$ cells were injected into P0+/+/MCP-1+/+, P0+/+/MCP-1-/-, P0+/-/MCP-1+/+ and P0+/-/MCP-1-/- mice which were previously irradiated sublethaly (5 Gy). Three months later mice were sacrificed and GFP+ leukocytes in blood smears were quantified to validate the chimerism. Only mice with more than 95% of leukocytes showing clear GFP-positivity were used for the analysis.

Quantification of GFP-positive and -negative macrophages was performed using nerves from transplanted P0+/+/MCP-1+/+ (n = 4), P0+/+/MCP-1-/- (n = 3), P0+/-/MCP-1+/+ (n = 4) and P0+/-/MCP-1-/- (n = 4) mice transcardially perfused with 4% PFA in PBS. Nerves were postfixed in the same solution for 2 h. Afterwards peripheral nerves were incubated in 10% sucrose in PBS overnight and frozen in O.C.T. matrix (DiaTec, Nürnberg, Germany). 10-µm-thick sections were used for immunohistochemical staining which were subsequentialy analysed with an Axioplan/Axiophot 2 fluorescence microscope (Zeiss, Göttingen, Germany).

4.11 *In-situ* hybridisation

In-situ hybridisation for the detection of MCP-1 mRNA was performed on sections of paraffin embedded femoral quadriceps, cutaneous saphenous and sciatic nerves from P0+/- and P0+/+ mice at the age of three and six months in collaboration with Dr. Marcus Müller, Department of Neurology, Westfälische Wilhelms-Universität, Münster, Germany (Campbell et al., 1994; Asensio et al., 1999).

P0+/+ and P0+/- mice were deeply anesthetized and transcardially perfused with PBS for five minutes followed by 4% PFA in PBS. Dissected sciatic, femoral quadriceps and cutaneous saphenous nerves were dehydrated, embedded in paraffin and cut into 5-µm-thick cross-sections. Sections of paraffin-embedded tissue were incubated with ^{33}P-labelled cRNA probes transcribed from linearized plasmid constructs containing the *ccl2* insert (target sequence see Appendix 7.5, Rollins et al., 1988) and processed for *in-situ* hybridisation combined with immunohistochemistry as described elsewhere (Campbell et al., 1994; Asensio et al., 1999).

Schwann cells were specifically detected by immunohistochemistry using a rabbit-anti-S100 antibody (DAKO Cytomation, Hamburg, Germany). Colorimetric detection was achieved by use of Vectastain ABC kits (Vector Laboratories, Burlingame, CA 94010, USA), and diaminobenzidine/H_20_2 reagent (Vector Laboratories, Burlingame, CA 94010, USA).

4.12 Ultrastructural analysis

Specimens of peripheral nerves (femoral nerves and lumbar ventral roots) for electron microscopy were generated as described elsewhere (Martini et al., 1995a; Martini et al., 1995b; Lindberg et al., 1999). Mice were anesthetized and transcardially perfused for five minutes with PBS followed by a 15 to 20 minute perfusion with 0.1 M cacodylate buffer, pH 7.4, substituted with 4% PFA and 2% glutaraldehyde. The tissue was subsequently postfixed over night in the same buffer, osmificated with 2% osmiumtetroxide in 0.1 M cacodylate buffer for two hours at room temperature, dehydrated in ascending acetone concentrations and embedded in Spurr`s medium (see Appendix 7.3).

Semithin section (0.5-µm-thick) were stained with alkaline methylene blue and analysed by light microscopy. Ultrathin sections (100 nm) were transferred on copper grids and treated

with lead citrate. Analysis was performed using a ProScan Slow Scan CCD camera (Lagerlechfeld, Germany) mounted to a Leo 906 E electron microscope (Zeiss, Oberkochen, Germany) and corresponding software iTEM (Olympus Soft Imaging Solutions GmbH, Münster, Germany). All sections were analysed by the investigator being not aware of the genotype.

4.13 MEK1/2-inhibition in P0 mice

P0+/+ and P0+/- mice were treated for three weeks with 100 mg per kg bodyweight of CI-1040 in DMSO gratefully provided by Pfizer, New York, USA. CI-1040 was administered by daily intraperitoneal injection of CI-1040 in DMSO. To achieve the right dosage per bodyweight with a maximal volume of 50 µl, a series of differently concentrated CI-1040 solutions were produced and mice were treated with appropriate solution after weighing. Mice losing weight and showing poor state of health after a few days due to the use of organic solvent were sacrificed at an early stage and not included in the study. Mice included in the study showed a good state of health. After injection mice got a short lasting (one to two minutes) paralysis of the hind limbs. All animal experiments were approved by the Regierung von Unterfranken.

4.14 Statistical analysis

Statistical analysis was performed by using the unpaired two-tailed Student's t test for comparison of macrophage and T-lymphocyte numbers, GFP-positive and GFP-negative CD68-positive macrophages per cross section and MCP-1 protein levels. Group differences in the analysis of foamy macrophages and neuropathological profiles were evaluated by use of the nonparametric Mann–Whitney U test. Differences revealed by qRT-PCR were evaluated by use of a Bonferroni corrected one-tailed ANOVA test. Statistical significance was supposed at $p \leq 0.05$.

5. Results

5.1. Functional role of MCP-1 in inherited peripheral neuropathies in P0+/- mice

Previous studies showed a significant increase in the total number of F4/80-positive macrophages from the age of four months onwards in the endoneurium of femoral quadriceps nerves of P0+/- mice in comparison to P0+/+ mice (Schmid et al., 2000). These macrophages are mainly considered as relevant for the demyelinating phenotype in P0+/- mice as they frequently are laden with myelin debris and can be located inside the endoneurial tube. In addition, a deficiency in M-CSF, an important macrophage-directed cytokine, leads to a decrease in the number of F4/80-positive macrophages and an ameliorated disease phenotype (Carenini et al., 2001; Ip et al., 2006).

To elucidate pathogenetic factors on a molecular level which might be necessary for an elevated infiltration, proliferation and/or activation of macrophages in myelin mutants, semi-quantitative real-time PCRs (qRT-PCRs) were applied to investigate the expression of macrophage-directed cytokines and chemokines in peripheral nerves of P0+/- mice in comparison to P0+/+ mice.

5.1.1. Early expression of MCP-1 by Schwann cells in peripheral nerves of P0+/- mice

Commercially available TaqMan assays for Interleukin-6 (IL-6), TNFα, M-CSF, GM-CSF, IFNγ, TGFβ, IL-1β and MCP-1 were performed using cDNA synthesized from femoral quadriceps, cutaneous saphenous and sciatic nerves` total RNA of P0+/+ and P0+/- mice at the age of one, three and twelve months in collaboration with Dr. Christoph Kleinschnitz, Department of Neurology, Julius-Maximilians-Universität, Würzburg, Germany.

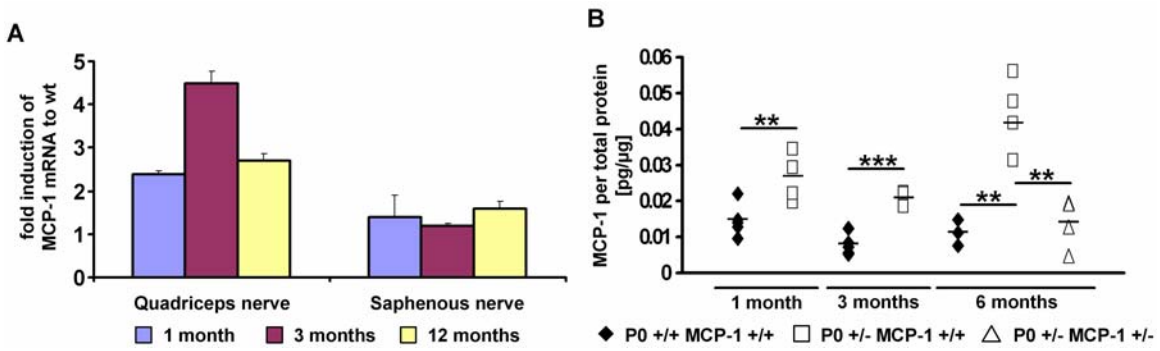

Figure 1: Quantification of MCP-1 mRNA and protein in femoral quadriceps nerves of P0+/+ and P0+/- mice.

(A) MCP-1 mRNA is expressed in peripheral nerves of P0+/- mice from the age of one month onwards. This expression is only significantly increased in femoral quadriceps nerves of P0+/- mice in comparison to nerves from P0+/+ nerves but not in cutaneous saphenous nerves. Shown are mean values plus SD. (**B)** An increased expression of MCP-1 protein is also evident in femoral quadriceps nerves from P0+/- mice in comparison to P0+/+ at the age of one, three and six months. Each symbol represents measured MCP-1 protein amount of femoral quadriceps nerves from one mouse. MCP-1 protein is expressed in similar amounts in femoral quadriceps nerves from P0+/-/MCP-1+/- as P0+/+ mice. Bars represent mean value. **p < 0.01; ***p < 0.001

A significant regulation of TNFα, TGFβ, IL-1β and IL-6 in femoral quadriceps nerves of one to six months old P0+/- mice was not detected but an elevation of M-CSF mRNA was observed from the age of six months onwards (not shown). The detected amount of MCP-1 mRNA in femoral quadriceps nerves is in contrast to all other examined cytokines already increased in P0+/- mice at the age of one month in comparison to P0+/+ mice (Figure 1A). In one month old P0+/- mice an almost 2.5 fold induction of MCP-1 mRNA in comparison to nerves from age-matched P0+/+ mice is detectable in femoral quadriceps nerves which lasts at least until the age of twelve months. In three months old mice the induction of MCP-1 mRNA is even higher (~4.5 fold induction). Similar results were achieved using cDNA from sciatic nerves.

As previously shown demyelination and accumulation of macrophages in peripheral nerves occur in femoral quadriceps nerves of P0+/- mice containing a quite high percentage of motor fibers (~40%) but not in sensory nerves like cutaneous saphenous nerves (Carenini et al., 2001). Furthermore, sensory nerves like the cutaneous saphenous nerves of P0+/- mice do not show any indication of a disease as in the femoral quadriceps nerves like thinly myelinated or demyelinated axons or an increase in immune cell number. Therefore, cutaneous saphenous nerves were additionally investigated by qRT-PCR regarding the amount of MCP-1 mRNA to clarify a putative correlation between MCP-1 expression and demyelinating disease (Figure 1A). In all investigated cutaneous saphenous nerves of P0+/- mice no or a non-significant elevated amount of MCP-1 mRNA was detected in comparison

to cutaneous saphenous nerves of age-matched P0+/+ mice showing a clear correlation between tissue, level of MCP-1 mRNA expression and demyelinating phenotype.

To verify the expression of MCP-1 in peripheral nerves of P0+/- mice in comparison to P0+/+ mice, the amount of MCP-1 protein was measured in sciatic, femoral quadriceps and cutaneous saphenous nerves by enzyme-linked immunosorbent assay (ELISA, Figure 1B). Similar to previous results all investigated femoral quadriceps nerves from P0+/- mice at the age of one, three and six months revealed a significant increased amount of MCP-1 protein per total protein in comparison to femoral quadriceps nerves of age-matched P0+/+ littermates. Femoral quadriceps nerves exhibit an average amount of 0.02 to 0.04 pg/µg and 0.01 pg/µg of MCP-1 protein per total protein for P0+/- and P0+/+ mice, respectively. The amount of MCP-1 protein in crushed sciatic nerves four days after injury in wild type mice used as positive control (Toews et al., 1998, data not shown) was about 0.03 pg/µg per total protein in the mean. Statistical analysis comparing MCP-1 protein amount per total protein in femoral quadriceps nerve of P0+/- to P0+/+ mice using a two-tailed student's T-test reveals p-values of < 0.01 for all age groups. Corroborating qRT-PCR data, an elevated amount of MCP-1 protein was not detected in cutaneous saphenous nerves of P0+/- mice in comparison to nerves from P0+/+ mice (not shown).

Expression of MCP-1 mRNA and protein in femoral quadriceps but not in cutaneous saphenous nerves of P0+/- and P0+/+ mice showed that the expression of MCP-1 spatial correlates with the demyelinating phenotype. Interestingly, although the amount of MCP-1 protein of peripheral nerves is quite low, MCP-1 mRNA and protein was also detected in nerves from P0+/+ mice showing a low but constitutive expression.

In a next step the cellular source of MCP-1 mRNA in peripheral nerves of P0+/+ and P0+/- mice was investigated in collaboration with Dr. Marcus Müller (Figure 2). For this purpose we performed an *in-situ* hybridisation on sections of paraffin embedded sciatic and femoral nerves of three and six months old P0+/- and P0+/+ mice using a ^{33}P-labeled riboprobe specific for MCP-1 mRNA. The detection of MCP-1 mRNA was combined with an immunohistochemical staining against S100β as a marker for Schwann cells. Sections from femoral quadriceps and sciatic nerves of P0+/+ mice and sections which were hybridized with a corresponding sense probe exhibit no silver granules which would show a specific staining for MCP-1 mRNA. In contrast, peripheral nerves from P0+/- mice show clear precipitation of silver granules representing MCP-1 expression. The overall staining was increased in peripheral nerves of six months old P0+/- mice in comparison to nerves from three months old P0+/+ mice.

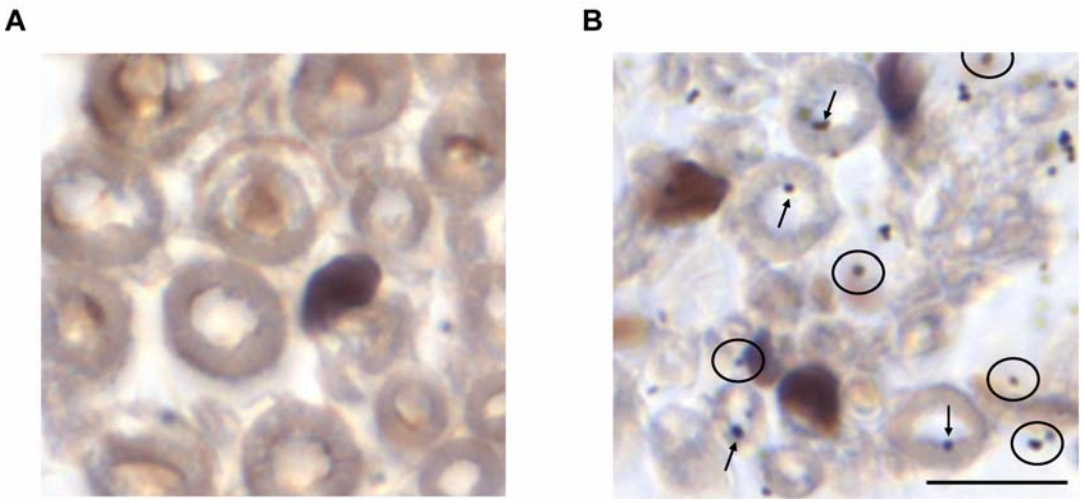

Figure 2: Cellular localisation of MCP-1 mRNA expression in peripheral nerves.
MCP-1 mRNA was detected using *in-situ* hybridisation in combination with immunhistochemistry against S100β as Schwann cell marker. Silver granules representing specific staining for MCP-1 mRNA were only visible in peripheral nerves from P0+/- mice (**B,** femoral quadriceps nerve shown) but not in nerves from P0+/+ mice (**A**) at the age of three (**A, B**) and six months (not shown). In femoral quadriceps nerves of three months old P0+/- mice specific granules (**B**) are connected with S100β–positiv staining (circles) and at Schwann cell-axon interface (arrows). Bar: 10 µm.

In sciatic and femoral quadriceps nerves of three and six months old P0+/- mice MCP-1 mRNA is detectable at the interface of Schwann cells and axons. In addition, MCP-1 specific silver granules were seen in association with S100β positive structures. Other endoneurial cells than Schwann cells and perineurial cells were not identified to be MCP-1 mRNA positive in nerves from three months old P0+/- mice. In contrast to this, other endoneurial cells than Schwann cells and perineurial cells were positive for MCP-1 mRNA specific silver granules in nerves of six months old P0+/- mice. Fibroblasts and macrophages which are present in the endoneurium are known to be potent to express immunological agents as e.g. MCP-1 (Taskinen and Roytta, 2000; Yoo et al., 2005).

qRT-PCR experiments identify MCP-1 as so far first known factor to be regulated in P0+/- mice as a model for CMT1B. The relevance of this finding is enforced by ELISAs and a combination of *in-situ* hybridisation and immunohistochemistry. All three techniques show a significant increase in the amount of MCP-1 mRNA and protein in femoral quadriceps but not in cutaneous saphenous nerves. Regarding these results and previous ones concerning the number of macrophages and the demyelinated phenotype in peripheral nerves of P0+/- (Schmid et al., 2000; Carenini et al., 2001) a correlation of MCP-1 expression and the occurrence of F4/80-positive macrophages in peripheral nerves of P0+/- in comparison to P0+/+ mice could be shown.

5.1.2. Deficiency of MCP-1 leads to reduced numbers of immune cells in the endoneurium of six months old P0+/- mice

To elucidate the function of MCP-1 in inherited peripheral neuropathies, P0+/- mice were crossbred with MCP-1 deficient mice (Lu et al., 1998) resulting in six different genotypes of P0/MCP-1 double mutant mice (P0+/+/MCP-1+/+, P0+/+/MCP-1+/-, P0+/+/MCP-1-/-, P0+/-/MCP-1+/+, P0+/-/MCP-1+/-, P0+/-/MCP-1-/-). Only littermates of double mutants and corresponding controls were analysed at the age of six months, an age at which a significant demyelinated phenotype and an elevated number of macrophages in P0+/- mice is supposed to be present, and twelve months, showing progressed demyelination in comparison to six months old P0+/- mice.

ELISA technique was used to investigate the expression of MCP-1 protein in peripheral nerves of the resulting double mutants (Figure 1B, page 27). Femoral quadriceps nerves from six months old P0+/-/MCP-1+/+ mice showed similar MCP-1 protein amounts as P0+/- mice from P0 single mutant mouse strain (0.036 ± 0.007 pg/µg total protein and ~0.041 ± 0.01 pg/µg total protein, respectively). As expected no MCP-1 protein was detectable in femoral quadriceps nerves from P0+/-/MCP-1-/- mice (data not shown) whereas nerves from P0+/-/MCP-1+/- mice showed an intermediate level of MCP-1 protein per total protein (0.014 ± 0.007 pg/µg) similar to P0+/+/MCP-1+/+ mice (P0+/-/MCP-1+/+ versus P0+/-/MCP-1+/-: $p < 0.01$). Similar results were previously shown for peritoneal macrophages of MCP-1+/- mice (Lu et al., 1998).

Figure 3A shows the total number of F4/80+ macrophages per section quantified in peripheral nerves from six months old P0/MCP-1 double mutant mice. In femoral quadriceps nerves of P0+/+ mice at the age of six months the number of F4/80+ macrophages was comparable regardless of the MCP-1 genotype and comparable to results achieved in previous studies (Schmid et al., 2000; Carenini et al., 2001). Furthermore, in all cutaneous saphenous nerves investigated no differences in macrophage numbers were apparent (data not shown). In sections of femoral quadriceps nerve of six months old P0+/-/MCP-1+/+ mice, the number of F4/80+ macrophages was comparable to numbers quantified in previous studies (11.2 ± 1.6, Schmid et al., 2000; Carenini et al., 2001). We also detected significantly elevated numbers in relation to femoral quadriceps nerves of P0+/+/MCP-1+/+ mice (4.7 ± 1.4; P0+/+/MCP-1+/+ versus P0+/-/MCP-1+/+: $p < 0.001$). In contrast to this, femoral quadriceps nerves of P0+/-/MCP-1+/- and P0+/-/MCP-1-/- mice exhibit significantly reduced

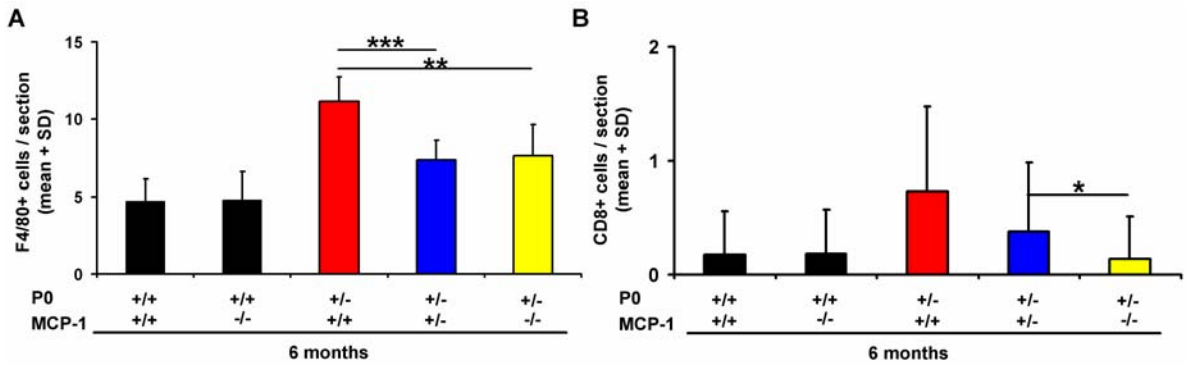

Figure 3: Quantification of F4/80–positive macrophages and CD8-positive T-lymphocyte in femoral quadriceps nerves of P0/MCP-1 double mutant mice.

(A) Quantification of F4/80–positive macrophages per section in femoral quadriceps nerves of six months old P0/MCP-1 mice exhibits decreased numbers of macrophages in nerves from MCP-1 deficient mice (P0+/-/MCP-1+/- and P0+/-/MCP-1-/-) in comparison to nerves from P0+/-/MCP-1+/+ mice. **(B)** Quantification of CD8–positive macrophages per section in femoral quadriceps nerves of six months old P0/MCP-1 mice. Reduced numbers of CD8–positive T-lymphocyte are obvious in nerves from P0+/-/MCP-1+/- and P0+/-/MCP-1-/- mice. *p < 0.05 **p < 0.01; ***p < 0.001.

numbers of F4/80-positive profiles in comparison to nerves from P0+/-/MCP-1+/+ mice (7.6 ± 2.1 and 7.2 ± 1.3 cells per section for P0+/-/MCP-1-/- and P0+/-/MCP-1+/-, respectively; P0+/-/MCP-1+/+ versus P0+/-/MCP-1+/- $p < 0.001$; P0+/-/MCP-1+/+ versus P0+/-/MCP-1-/- $p < 0.01$). P0+/-/MCP-1+/- and P0+/-/MCP-1-/- mice still harbour slightly, but non-significantly more macrophages in the mean in the endoneurium of femoral quadriceps nerves than P0+/+ mice.

The amount of endoneurial CD8-positive cells in femoral quadriceps nerves followed the same tendency (Figure 3B). Similar to results achieved in previous studies (Schmid et al., 2000) femoral quadriceps nerves of P0+/-/MCP-1+/+ mice exhibit significant more CD8-positive profiles than P0+/+/MCP-1+/+ mice (0.73 ± 0.53 and 0.17 ± 0.07, respectively; Figure 3B). In addition, it is obvious that in six months old mice the amount of CD8-positive lymphocytes per section of femoral quadriceps nerves was lower in P0+/-/MCP-1+/- (0.38 ± 0.23) and P0+/-/MCP-1-/- (0.14 ± 0.2) mice in comparison to P0+/-/MCP-1+/+ mice. Thereby, P0+/-/MCP-1+/- exhibited a significant higher amount of CD8-positve T-lymphocytes per nerve section than P0+/-/MCP-1-/- ($p < 0.05$).

In summary, a deficiency for MCP-1 either heterozygously or homozygously leads to decreased numbers of macrophages and CD8-positive T-lymphocytes in femoral quadriceps nerves of six months old P0+/- mice.

5.1.3. MCP-1 deficiency leads to a reduced immigration of macrophages into peripheral nerves

Our group has previously shown that during aging in nerves of P0+/- mice the number of macrophages increases significantly. Using bone marrow chimeric mice which received GFP-positive bone marrow and were sacrificed four months after transplantation showed that the proportion of GFP-positive macrophages is around 60% in P0+/+ and P0+/- mice (Maurer et al., 2003). This probably reflects a turnover of resident macrophages in peripheral nerves and hematogenous macrophages as already previously observed in rats (Vass et al., 1993).

To further study the impact of MCP-1 on the occurrence of macrophages in the endoneurium, GFP+ bone marrow chimeras were generated using P0+/+/MCP-1+/+, P0+/+/MCP-1-/-, P0+/-/MCP-1+/+ and P0+/-/MCP-1-/- mice. The success of bone marrow transplantation and chimerism of mice was evaluated by quantifying the percentage of GFP-positive leukocytes in blood smears of transplanted mice**.** Five mice out of 19 showed a percentage of GFP-positive leukocytes less then 95% and were not subjected to analysis.

The number of CD68+ macrophages in P0+/+/MCP-1+/+ and P0+/-/MCP-1+/+ mice per section of femoral quadriceps and cutaneous saphenous nerves was comparable to previously quantified numbers (see Figure 4, Maurer et al., 2003). It was also obvious in this experiment that P0+/+/MCP-1+/+ and P0+/+/MCP-1-/- mice exhibit similar numbers of CD68-positive macrophages per section of femoral quadriceps nerve as shown above (6.44 ± 2.38 and 6.61 ± 0.65, respectively). In comparison to that, femoral quadriceps nerves of P0+/-/MCP-1+/+ mice showed a significant elevation of macrophage number whereas sections of nerves from P0+/-/MCP-1-/- mice showed only a small increase in the total amount of macrophages in comparison to P0+/+ mice (11.13 ± 1.77 and 8.43 ± 1.70, respectively). These results are comparable to results achieved in non-transplanted P0 mice as shown in the previous section.

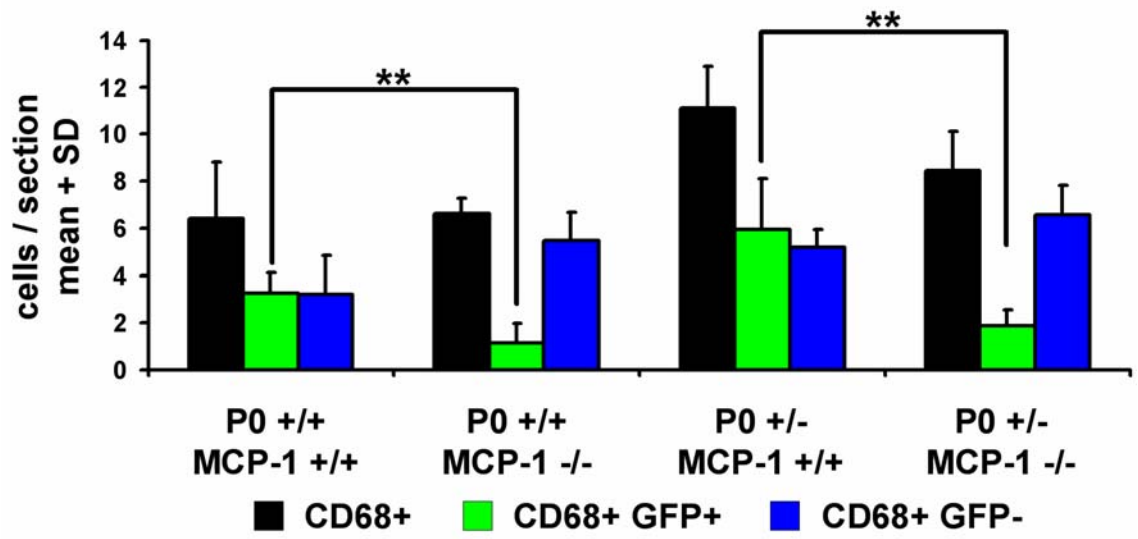

Figure 4: Quantification of GFP- and GFP+ CD68–positive macrophages in femoral quadriceps nerves of P0/MCP-1 double mutant mice.

The number of GFP+ macrophages in peripheral nerves is significantly reduced in the absence of MCP-1 (P0+/+/MCP-1-/- and P0+/-/MCP-1-/- mice). The reduction of GFP+ macrophages represents the lowered total number of macrophages in the endoneurium of nerves from P0+/-/MCP-1-/- mice. **p < 0.01.

Quantification of the percentage of GFP-positive macrophages in relation to the total number of macrophages showed the account of MCP-1 on the occurrence of macrophages into the endoneurium of investigated nerves. Femoral quadriceps nerves of mice not deficient for MCP-1, P0+/+/MCP-1+/+ and P0+/-/MCP-1+/+ mice, exhibited around 50% GFP-positive CD68-positive macrophages (3.25 ± 0.89 and 5.96 ± 2.16 for P0+/+/MCP-1+/+ and P0+/-/MCP-1-/-, respectively). Contrary femoral quadriceps nerves from mice homozygously deficient for MCP-1, P0+/+/MCP-1-/- and P0+/-/MCP-1-/- mice, showed much lower numbers of GFP/CD68-double positive macrophages (17% and 20% or 1.14 ± 0.84 and 1.86 ± 0.70, respectively; P0+/+/MCP-1+/+ versus P0+/+/MCP-1-/- $p = 0.016$; P0+/-/MCP-1+/+ versus P0+/-/MCP-1-/- $p = 0.01$). Therefore, peripheral nerves of MCP-1 deficient mice showed less GFP-positive macrophages as nerves from MCP-1 wild type mice regardless of P0 genotype suggesting that the infiltration of macrophages into the endoneurium was diminished due to the absence of MCP-1. This data clearly depicts that the infiltration of macrophages into the endoneurium of femoral quadriceps nerves is reduced in MCP-1 deficient mice.

P0+/-/MCP-1-/- and especially P0+/+/MCP-1-/- GFP bone marrow chimeras exhibited a higher proportion of GFP-negative CD68-positive macrophages in the endoneurium. This higher number of GFP-CD68+ macrophages may represent a longer retention period in the peripheral nervous tissue or enhanced proliferation of these cells.

5.1.4. Heterozygous, but not homozygous MCP-1 deficiency ameliorates the genetically mediated demyelinating disease in peripheral nerves of P0+/- mice

To further elucidate the impact of MCP-1 on the pathogenesis, morphometric studies on ultrastructural level using electron microscopy were accomplished quantifying pathological alterations in peripheral nerves of P0+/-/MCP-1+/+, P0+/-/MCP-1+/- and P0+/-/MCP-1-/- mice in comparison to P0+/+/MCP-1+/+, P0+/+/MCP-1+/- and P0+/+/MCP-1-/- mice. In femoral quadriceps nerves and lumbar ventral roots several different pathological alteration like thinly myelinated and demyelinated axons, degenerated axons, periaxonal vacuoles and onion bulbs were quantified.

Nerves of six and twelve months old P0+/+ mice showed no pathological alterations irrespective of MCP-1 genotype. Peripheral nerves of six months old P0+/-/MCP-1+/+ mice showed clear pathological alterations as P0+/- mice. In comparison to peripheral nerves of six months old P0+/- single mutant mice nerves from P0+/-/MCP-1+/+ mice showed less pathological alterations which might be due to differences in genetic background. The investigation of femoral quadriceps nerves and lumbar ventral roots of six months old P0+/-/MCP-1+/+, P0+/-/MCP-1+/- and P0+/-/MCP-1-/- mice revealed no obvious differences regarding morphology.

Concerning normal and abnormal myelinated nerve fibers, striking differences were visible between peripheral nerves of P0+/-/MCP-1+/+, P0+/-/MCP-1+/- and P0+/-/MCP-1-/- mice at the age of twelve months (Figure 5). Lumbar ventral roots of P0+/-/MCP-1+/+ mice exhibited demyelinated and thinly myelinated fibers which were prominently present throughout the endoneurium. Lumbar ventral roots from P0+/-/MCP-1+/- mice instead showed less thinly myelinated fibers and only a few totally demyelinated axons. Whereas the presence of thinly myelinated axons was similar in lumbar ventral roots of P0+/-/MCP-1+/+ and P0+/-/MCP-1-/- mice the number of demyelinated axons was even higher in ventral roots of P0+/-/MCP-1-/- mice (Figure 5). Quantifying the amount of normal myelinated axons as well as thinly myelinated and demyelinated axons (Figure 6) revealed significant differences between P0+/-/MCP-1+/+, P0+/-/MCP-1+/- and P0+/-/MCP-1-/- mice in femoral quadriceps nerves and lumbar ventral roots.

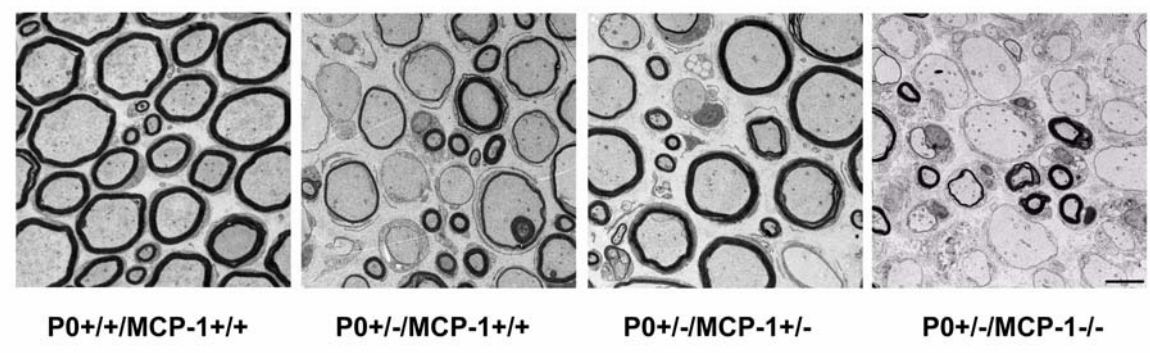

Figure 5: Electron micrographs of lumbar ventral roots of twelve months old P0/MCP-1 double mutant mice.

In comparison to lumbar ventral roots of twelve months old P0+/+/MCP-1+/+ mice the typical picture of a demyelinating disease is obvious in nerves from P0+/-/MCP-1+/+ mice. In lumbar ventral roots from P0+/-/MCP-1+/- mice a significant amelioration of the disease can be seen due to the presence of almost normal myelinated fibers and decreased number of thinly and demyelinated fibers. In contrast to this, lumbar ventral roots of P0+/-/MCP-1-/- mice exhibit an aggravation of disease in comparison to nerves from P0+/-/MCP-1+/- mice. Bar: 5µm.

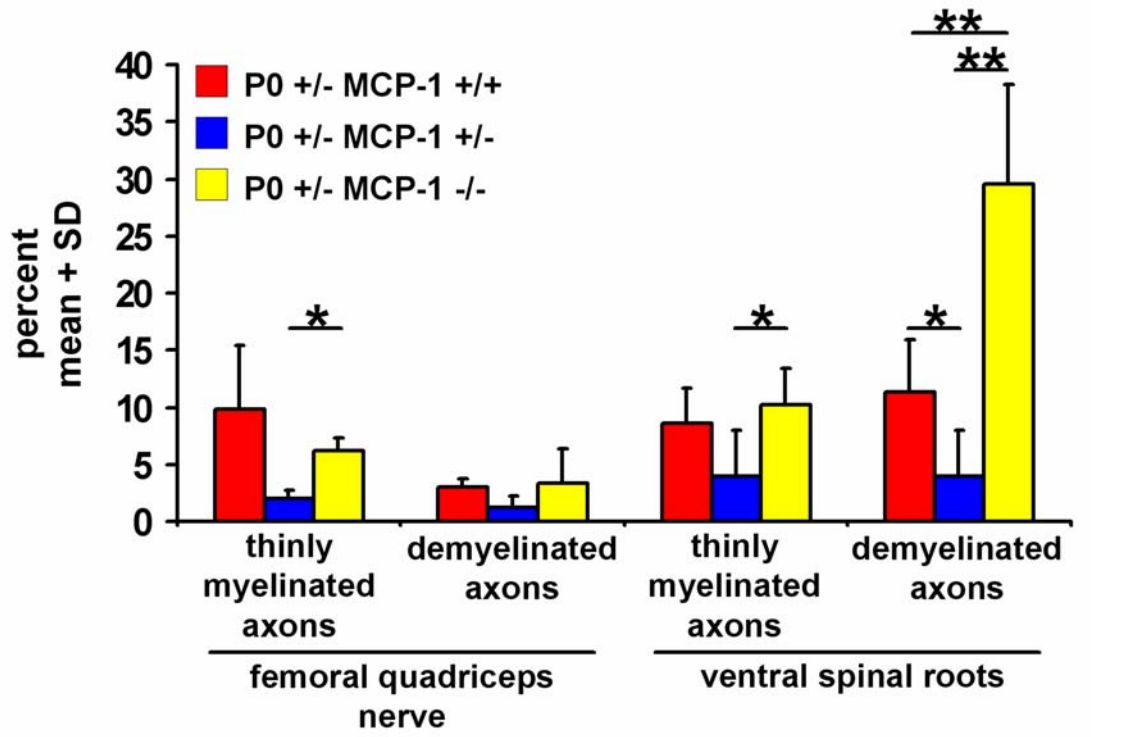

Figure 6: Quantification of pathological alteration in peripheral nerves from P0/MCP-1 double mutant mice.

At the age of twelve months the amount of thinly and demyelinated nerve fibers is decreased in femoral quadriceps nerve and ventral spinal roots of P0+/-/MCP-1+/- mice in comparison to nerves from P0+/-/MCP-1+/+ mice reflecting a strong amelioration of pathology. Contrary, peripheral nerves from P0+/-/MCP-1-/- showed no amelioration of disease in comparison to nerves from P0+/-/MCP-1+/+ and even higher numbers of demyelinated nerve fibers in lumbar ventral roots. *$p < 0.05$; **$p < 0.01$.

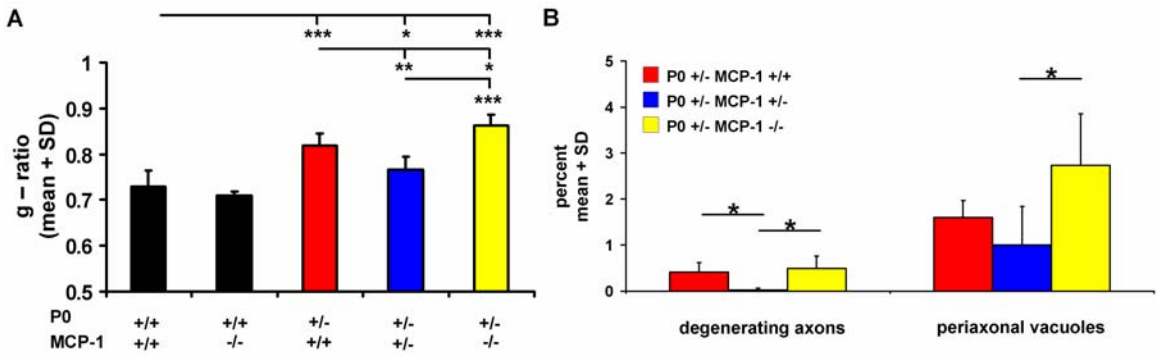

Figure 7: Quantification of g-ratio and axonopathic changes in lumbar ventral roots from P0/MCP-1 double mutant mice.

(A) Quantifying the g-ratio in lumbar ventral roots of P0/MCP-1 mice confirm an amelioration of the demyelinating phenotype in P0+/-/MCP-1+/- mice, whereas thinner myelin sheaths in nerves from P0+/-/MCP-1-/- mice confirm an aggravation of the disease.

(B) Additionally, axonopathic changes, like periaxonal vacuoles are reduced in peripheral nerves from P0+/-/MCP-1+/- and increased in nerves from P0+/-/MCP-1-/- mice. *p < 0.05; **p < 0.01; ***p < 0.001.

Another option to quantify and evaluate the myelination of axons in peripheral nerves is to determine the g-ratio which is defined as quotient of axon circumference and corresponding myelin circumference. Adult myelinated nerve fibers of mice typically exhibit a g-ratio of around 0.73. Figure 7A depicts that in the mean lumbar ventral roots of P0+/-/MCP-1+/- resemble an almost normal myelinated peripheral nerve (0.77 ± 0.03) in comparison to P0+/+/MCP-1+/+ nerves (0.73 ± 0.04). Peripheral nerves from P0+/-/MCP-1+/+ and P0+/-/MCP-1-/- mice showed clearly higher g-ratio (0.82 ± 0.03 and 0.86 ± 0.02, respectively) and so thinner myelin sheaths in the mean.

In addition to an ameliorated demyelinating phenotype in peripheral nerves of P0+/-/MCP-1+/- mice a reduced degree of axonopathic alterations (Figure 7B) at least in lumbar ventral roots was observed. Typical morphological indicators for an ongoing axonopathy are the presence of degenerated axons, periaxonal vacuoles as a sign of axonal degeneration and loss of axons represented by reduced total number of axons. A loss of axons could not be detected in lumbar ventral roots. The number of degenerated axons in lumbar ventral roots of P0+/-/MCP-1+/- mice (0.02%) was significantly reduced in comparison to roots from P0+/-/MCP-1+/+ and P0+/-/MCP-1-/- mice (0.31% and 0.44%, respectively; P0+/-/MCP-1+/- versus P0+/-/MCP-1+/+ and P0+/-/MCP-1-/-: $p < 0.05$). On the other hand periaxonal vacuoles were increased in ventral lumbar roots of P0+/-/MCP-1-/- mice.

In femoral quadriceps nerves of P0+/-/MCP-1+/+, P0+/-/MCP-1+/- and P0+/-/MCP-1-/- the proportion of degenerated axons and periaxonal vacuoles was similar regardless of MCP-1 genotype. This might be due to a more progressed disease in femoral quadriceps nerves in comparison to lumbar ventral roots leading to non-detectable morphological differences between femoral quadriceps nerves of P0+/-/MCP-1+/+ , P0+/-/MCP-1+/- and P0+/-/MCP-1-/-.

In summary, myelination in peripheral nerves of P0+/-/MCP-1+/- mice was best restored and indicators for an axonopathy were only scarcely found. Peripheral nerves of P0+/-/MCP-1-/- mice instead showed no amelioration and even an aggravation of disease in lumbar ventral roots in comparison to nerves of P0+/-/MCP-1+/+ mice.

5.1.5. Peripheral nerves of twelve months old heterozygous and homozygous MCP-1 deficient P0+/- mice exhibit significant differences in immune cell number and cytokine expression

Due to the differences in morphology of peripheral nerves of P0+/-/MCP-1+/- and P0+/-/MCP-1-/- mice several approaches were applied to further characterise the disease course in these mice. Quantification of immune cells in peripheral nerves of twelve months old mice revealed a different situation than in six months old mice. In femoral quadriceps nerves of twelve months old mice differences in the number of CD8-positive cells per nerve section between P0+/-/MCP-1+/+ and P0+/-/MCP-1-/- were not obvious as in six months old mice (1.97 ± 1.61 cells/section and 1.44 ± 0.86, respectively, Figure 8A). P0+/-/MCP-1+/+ and P0+/-/MCP-1-/- clearly showed increased numbers of CD8+ T-lymphocytes in comparison to nerves from P0+/+/MCP-1+/+ and P0+/+/MCP-1-/- mice (0.2 ± 0.2 and 0.14 ± 0.15, respectively). Femoral quadriceps nerves of twelve months old P0+/-/MCP-1+/- mice harbour significant lower numbers of CD8+ T-lymphocytes (1.02 ± 0.98 cells/section) in comparison to P0+/-/MCP-1-/- mice ($p < 0.05$).

Interestingly, the quantification of CD4-positive T-lymphocytes per section of femoral quadriceps nerve revealed highest number of CD4-positive T-Lymphocytes (Figure 8B) in nerves from P0+/-/MCP-1+/- mice (0.79 ± 0.18 cells per section). The numbers of CD4+ T-lymphocytes in femoral quadriceps nerves of P0+/-/MCP-1+/+ and P0+/-/MCP-1-/- mice were similar but lower than in nerves from P0+/-/MCP-1+/- (0.21 ± 0.19 and 0.29 ± 0.12 cells

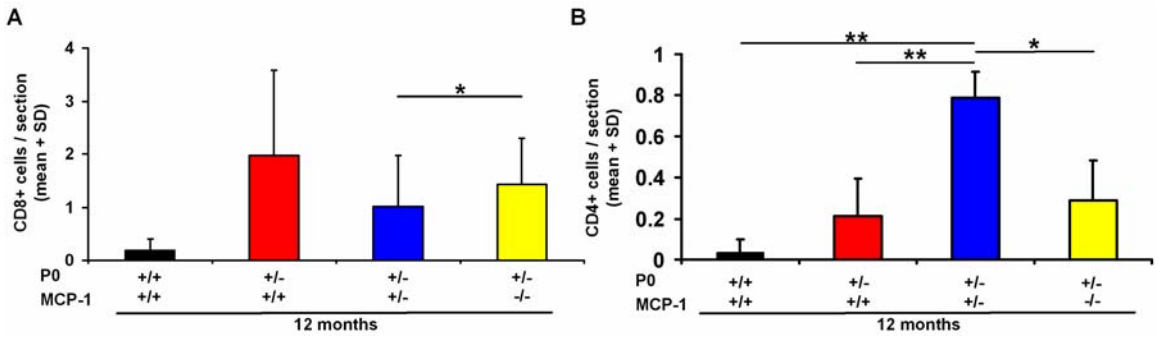

Figure 8: Quantification of CD8–positive and CD4–positive T-lymphocytes in femoral quadriceps nerve of twelve months old P0/MCP-1 double mutant mice.

(A) Quantification of CD8–positive T-lymphocytes per section in femoral quadriceps nerves of twelve months old P0/MCP-1 mice. Reduced numbers of CD8–positive T-lymphocyte are obvious in nerves from P0+/-/MCP-1+/-. **(B)** Quantification of CD4-positive T-lymphocytes per section in femoral quadriceps nerves of twelve months old P0/MCP-1 double mutant mice revealed an increased amount of CD4–positive cells in P0+/-/MCP-1+/- mice. *p < 0.05 **p < 0.01; ***p < 0.001.

per section respectively, P0+/-/MCP-1+/+ versus P0+/-/MCP-1+/- $p < 0.01$; P0+/-/MCP-1+/- versus P0+/-/MCP-1-/- $p < 0.05$). The total number of CD4+ T-lymphocytes per nerve section quantified is very low but similar to quantifications of CD4+ T-lymphocytes in peripheral nerves by co-workers (Antje Kroner and Bianca Kohl, unpublished observations).

Analysis of macrophage numbers in femoral quadriceps nerves of P0+/-/MCP-1+/+ mice shows approximately 2.6 fold more macrophages than in nerves from P0+/+/MCP-1+/+ mice (19.6 ± 1.5 and 7.4 ± 1.1, respectively; p-value < 0.001, Figure 9A). Nerves of P0+/-/MCP-1-/- mice exhibited an average of 14.4 ± 1.2 macrophages per nerve section which signifies a small, but non-significant reduction of F4/80-positive cells per nerve section. Femoral quadriceps nerves from P0+/-/MCP-1+/- mice exhibit 8.6 ± 2.9 and thus a significantly reduced number of endoneurial macrophages in comparison to P0+/-/MCP-1+/+ and P0+/-/MCP-1-/- (P0+/-/MCP-1-/- to P0+/-/MCP-1+/-: p-value < 0.01; P0+/-/MCP-1+/- to P0+/-/MCP-1+/+: p-value < 0.001).

In femoral quadriceps nerves but also in lumbar ventral spinal roots of twelve months old mice the number of foamy macrophages was additionally investigated by electron microscopy (Figure 9B). Foamy macrophages are macrophages which obviously phagocytosed material and exhibit large collections of vesicles within their cytoplasm. In peripheral nerves showing a demyelinating phenotype foamy macrophages are characterised by vesicles containing large membranous and therefore most probable myelin debris. The quantification of foamy macrophages in peripheral nerves of P0+/-/MCP-1-/- mice revealed higher numbers than in nerves from P0+/-/MCP-1+/+ mice (0.83 ± 0.56 versus 0.46

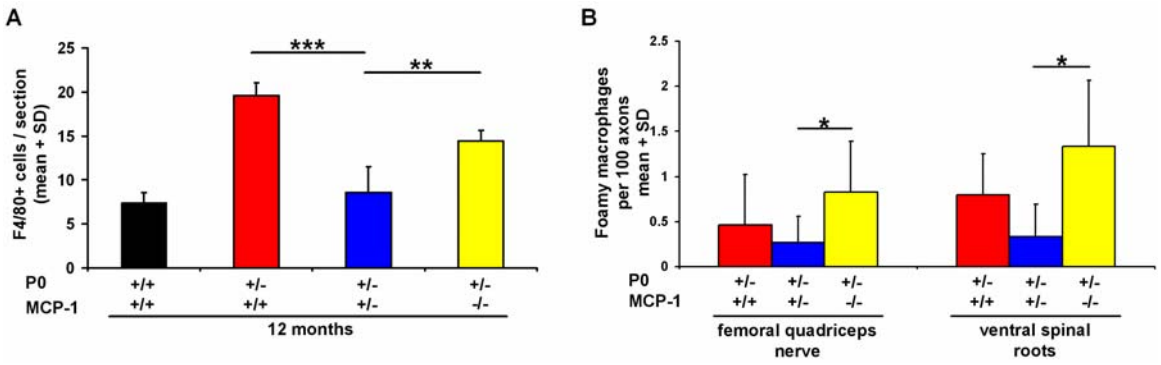

Figure 9: Quantification of F4/80–positive macrophages and foamy macrophages from P0/MCP-1 mice at the age of 12 months.

(A) Quantification of F4/80–positive macrophages per section in femoral quadriceps nerves of twelve months old P0/MCP-1 mice revealed siginificantly reduced macrophage numbers in nerves from P0+/-/MCP-1+/- mice and only slightly reduced numbers in nerves from P0+/-/MCP-1-/- mice. **(B)** Quantification of foamy macrophages per section in femoral quadriceps nerves of twelve months old P0/MCP-1 double mutant mice. Number of foamy macrophages in peripheral nerves from P0+/-/MCP-1-/- mice is significantly decreased whereas higher numbers are present in nerves from P0+/-/MCP-1-/- in comparison to nerves from P0+/-/MCP-1+/+ mice although nerves from P0+/-/MCP-1-/- exhibit slightly decreased total number of macrophages **(A)**. *$p < 0.05$ **$p < 0.01$; ***$p < 0.001$.

± 0.56 foamy macrophages per 100 axons in femoral quadriceps nerves, respectively; 1.34 ± 0.72 versus 0.79 ± 0.46 foamy macrophages per 100 axons in lumbar ventral roots, respectively). Furthermore, peripheral nerves of P0+/-/MCP-1+/- mice exhibited reduced numbers of foamy macrophages compared to nerves from P0+/-/MCP-1+/+ mice (0.27 ± 0.29 in femoral quadriceps nerves; 0.33 ± 0.36 in lumbar ventral roots; P0+/-/MCP-1+/- versus P0+/-/MCP-1-/-: $p < 0.05$).

Additionally, the cytokine milieu which might be related to macrophage activation seemed to be different in the examined nerves (Figure 10). One important mediator for survival, proliferation and differentiation of tissue macrophages is M-CSF (Cecchini et al., 1994; Pixley and Stanley, 2004; Chitu and Stanley, 2006) which seems to play a substantial role in the pathogenesis of the myelin mutants investigated so far in our institute. Therefore, we investigated the expression of M-CSF on mRNA and protein level by qRT-PCR and ELISA in lumbar ventral roots of twelve months old mice. The M-CSF mRNA expression level in lumbar ventral roots of P0+/-/MCP-1-/- mice was increased in comparison to nerves of P0+/+/MCP-1+/+, P0+/+/MCP-1-/-, P0+/-/MCP-1+/+ and P0+/-/MCP-1+/- mice (Figure 10A). Further evaluation revealed that higher concentrations of M-CSF protein per total protein were also present in P0+/-/MCP-1-/- (Figure 10B).

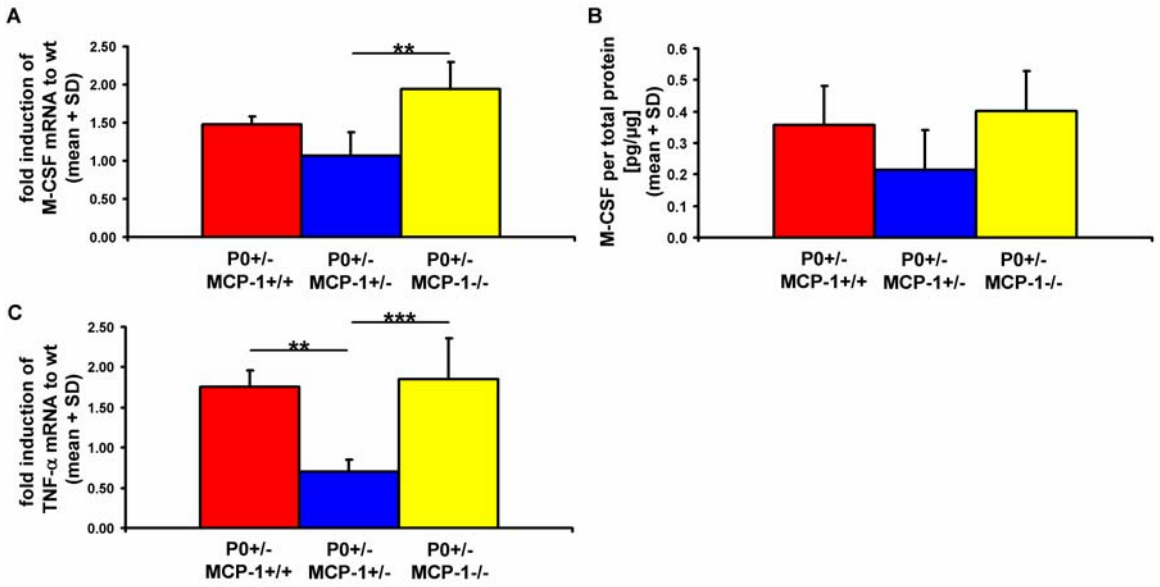

Figure 10: Quantification of cytokine mRNA and protein expression in lumbar ventral roots of P0/MCP-1 double mutant mice.

In comparison to peripheral nerves from P0+/-/MCP-1+/+ and P0+/-/MCP-1-/- mice nerves from P0+/-/MCP-1+/- mice showed reduced expression of M-CSF mRNA **(A)**, protein **(B)** and TNFα mRNA **(C)**. **p < 0.01; ***p < 0.001

Another hint for the induction of a more active or inflammatory phenotype of macrophages in lumbar ventral roots of P0+/-/MCP-1-/- was a significantly increased amount of TNFα mRNA (Figure 10C) and slightly increased levels of IL-1β and IL-6 mRNA in peripheral nerves of P0+/-/MCP-1-/- mice. In lumbar ventral roots of six months old P0+/-/MCP-1+/- mice a non-significantly increased expression of anti-inflammatory IL-10 was found.

5.2. Regulation of MCP-1 in peripheral nerves of P0+/- mice

Having identified MCP-1 as an early induced cytokine in an animal model for CMT1B with a crucial function in pathogenesis and pathological outcome, we further investigated regulatory mechanisms which might be relevant for MCP-1 induction and therefore might also be interesting as molecular targets for therapeutical approaches.

5.2.1. Activated signalling kinases in peripheral nerves of P0 mutants

Due to the important role of MCP-1 in the pathogenesis of a wide range of diseases (Dawson et al., 2003) like atherosclerosis (Braunersreuther et al., 2007), multiple sclerosis (Gonzalez-Amaro and Sanchez-Madrid, 2002) and rheumatoid arthritis (Feldmann et al., 1995) regulation of transcription of *ccl2,* the gene encoding for MCP-1, has been intensively investigated. Several studies elucidated the regulatory elements of *ccl2* which are downstream of p38 mitogen-activated protein kinase (MAPK, Sheng et al., 2005; Ip et al., 2006), IκBα/NFκB-signalling (Goebeler et al., 2001), JNK-signalling (Waetzig et al., 2005), PI3K/Akt-signalling (Yoo et al., 2005; Venkatesan et al., 2006), STAT1α (Venkatesan et al., 2006) and MEK1/2-ERK1/2-signalling (Boekhoudt et al., 2003; Yoo et al., 2005; Ip et al., 2006; Cramer et al., 2008). To clarify the activation status of signalling cascades which might be relevant for the induction of MCP-1 expression in peripheral nerves of P0+/- mice phosphorylation specific antibodies were used for Western blot analyses.

Investigating activation of Akt revealed no obvious differences between peripheral nerves of P0+/+ and P0+/- mice. In case of p38-signalling no signal at all was detectable for phosphorylated p38. This might be due to a low amount of these kinases at all in peripheral nerves (see Figure 11A). Examinations of the phosphorylation of JNK1/2/3 (Figure 11B), IκBα (Figure 11C) and the activation/translocation of p65 (not shown) lead to the conclusion that none of this signalling cascades were differently activated in nerves of one to six months old P0+/- mice in comparison to nerves from P0+/+ mice. In addition no activation was observed for STAT1α and STAT3 in one month old mice. Femoral quadriceps nerves from three months old P0+/- mice showed a slight increase in the phosphorylation of STAT1α (Figure 11D).

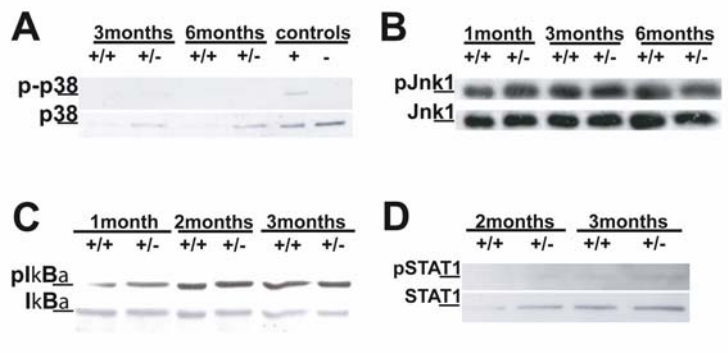

Figure 11: Western blot analyses revealed no obvious differences in most investigated signalling pathways between peripheral nerves from P0+/+ and P0+/- mice.

Examples are shown for some investigated signalling pathways. **(A)** Phospho-p38 was not detected in peripheral nerves. Signalling proteins like JNK1 **(B)** and NFκB related proteins in one to six months like IκBα **(C)** or p65 (not shown) did not show any differences in peripheral nerve protein lysates from P0+/+ and P0+/- mice. Other signalling kinases were either not phosphorylated like p38 **(A)** or activated to later time points like STAT1 **(D)**.

Sciatic and femoral quadriceps nerves of one month old P0+/- mice showed an increase in phosphorylated ERK1/2 proteins in comparison to nerves from P0+/+ mice (Figure12A). Strong phosphorylation of ERK1/2 was evident in three and six months old P0+/- mice which supports a sustained activation of this signalling cascade. In cutaneous saphenous nerves where no pathological alterations occur in older mice, no significant differences in the phosphorylation of the ERK1/2 in P0+/- and P0+/+ mice were visible (Figure12B). To further characterise the activation status of the ERK1/2 cascade, upstream kinases of ERK1/2, namely MAPK-ERK-kinase1/2 (MEK1/2), were investigated. MEK1/2 are more phosphorylated in femoral quadriceps nerves of P0+/- mice than in nerves of P0+/+ mice which could be shown at least for three and six months old mice (Figure 12C).

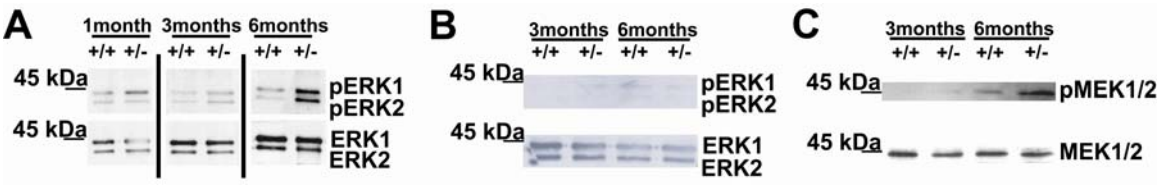

Figure 12: Western blot analysis of the MEK1/2-ERK1/2 signalling cascade by use of phosphorylation-specific antibodies.

(A) In femoral quadriceps nerves of one, three and six months old P0+/- mice increased phosphorylation of ERK1/2 in comparison to nerves from P0+/+ is obvious. **(B)** Evaluation of ERK1/2 phosphorylation in cutaneous saphenous nerves of same animals as **(A)** showed no differences between nerves from P0+/+ and P0+/- mice. **(C)** The direct upstream kinases of ERK1/2, namely MEK1/2, also showed increased phosphorylation level in femoral quadriceps nerves from P0+/- mice in comparison to P0+/+ mice similar to phosphorylation of ERK1/2.

In summary, the MEK1/2-ERK1/2-cascade showed an activation status in femoral quadriceps nerves and sciatic nerves but not in cutaneous saphenous nerves from one month onwards in P0+/- mice in comparison to nerves from P0+/+ mice and all other investigated signalling cascades. Therefore, an interrelationship between the MCP-1 expression and the activation of MEK1/2-ERK1/2 signalling might exist.

5.2.2 Activated ERK1/2 kinases are temporarily and spatially present at sites of MCP-1 expression

To further investigate a putative role of the activated MEK1/2-ERK1/2-cascade in the regulation of MCP-1 in peripheral nerves of P0+/- mice the localisation of phosphorylated ERK1/2 kinases in the endoneurium was examined to clarify a potential temporary and spatial colocalisation within cells expressing MCP-1, namely Schwann cells. Cross sections and single nerve fiber preparations were stained against phosphorylated ERK1/2 proteins and different markers of endoneurial cell types.

In femoral quadriceps nerves of one month old mice phosphorylated ERK1/2 proteins were almost exclusively found in Schwann cells of P0+/- mice (Figure 13A, B). The phosphoERK1/2-positiv profiles mainly showed a crescent morphology as typical for myelinating Schwann cells and were associated to S100β-positive profiles. Quantification of phosphoERK1/2-positive nuclei in the endoneurium showed a significantly elevated number of phosphoERK1/2-positive nuclei in P0+/- mice in comparison to P0+/+ already in one month old mice, whereas the total number of nuclei was similar (Figure 13C, D). Comparable results were achieved in three and twelve months old mice.

Frequently, specific staining for phosphorylated ERK1/2 proteins was supposed to be perinuclear or nuclear in cross sections of peripheral nerves. Using confocal laser scanning microscopy of single nerve fiber preparations of femoral quadriceps nerves showed indeed a clear staining specific for phosphorylated ERK1/2 proteins in Schwann cell nuclei of P0+/- mice whereas phosphoERK1/2-positivity was almost absent in Schwann cells from P0+/+ mice and only rarely nuclear (Figure 13E, F).

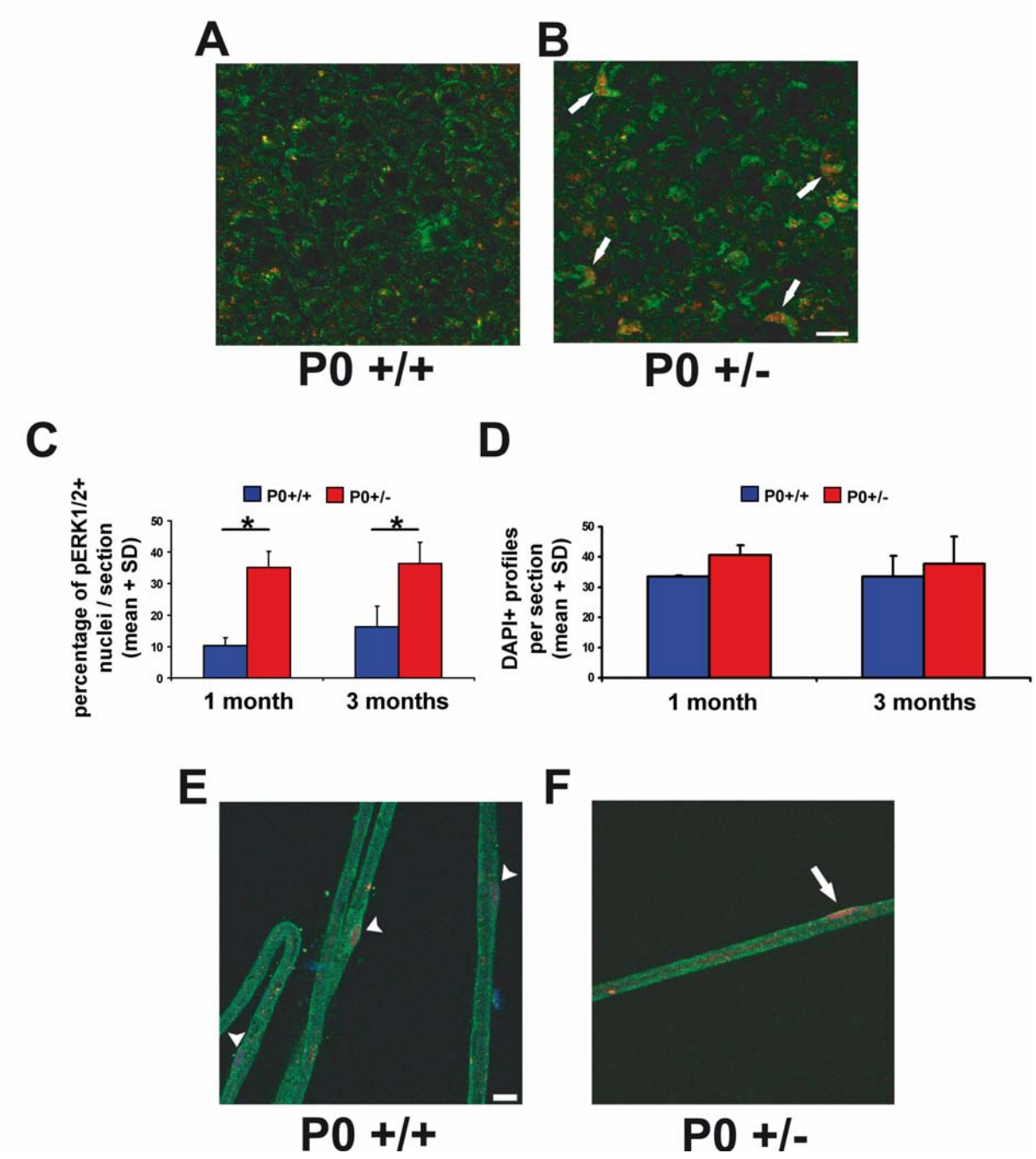

Figure 13: Activated ERK1/2 is mainly present in nuclei of myelinating Schwann cells in P0+/- mice.

In comparison to nerves from P0+/+ mice **(A)** femoral quadriceps nerves of P0+/- mice **(B)** showed an enrichment of phosphoERK1/2-positive (**red**) Schwann cells (**S100β**). Note the typical crescent structure for cell bodies of myelinating Schwann cells stained for phosphoERK1/2 in (B). In femoral quadriceps nerves from P0+/- mice an increased percentage of nuclei are phosphoERK1/2-positive **(C)** without obvious differences in total number of cells **(D)**. **(E, F)** Using confocal laser scanning microscopy clearly shows that phosphoERK1/2-positivity is located in Schwann cell nuclei in peripheral nerves of P0+/- mice **(F)** but not in nerves of P0+/+ mice (**E;** Bars in B and F: 10µm**).**

These immunohistochemical investigations revealed that phosphorylation of ERK1/2 and expression of MCP-1 do not only temporary overlap but also occur in the same cell type, mutant myelinating Schwann cells, carrying the primary defect.

5.2.3 Inhibition of the MEK1/2-ERK1/2 cascade in vitro leads to reduced expression of MCP-1 in Schwann cells

As a first approach to test if the MEK1/2-ERK1/2 cascade might be able to induce the expression of MCP-1 in Schwann cells an established Schwann cell line was investigated in analogy to Tofaris and colleagues (Tofaris et al., 2002). The Schwannoma cell line Rn22 was cultured in DMEM supplemented with 10% FCS. In all tested conditions a clear expression of MCP-1 on mRNA and protein level was obvious (Figure 14A, B,). Further investigation showed additionally that Rn22 cells exhibit phosphorylated ERK1/2 proteins (Figure 14C).

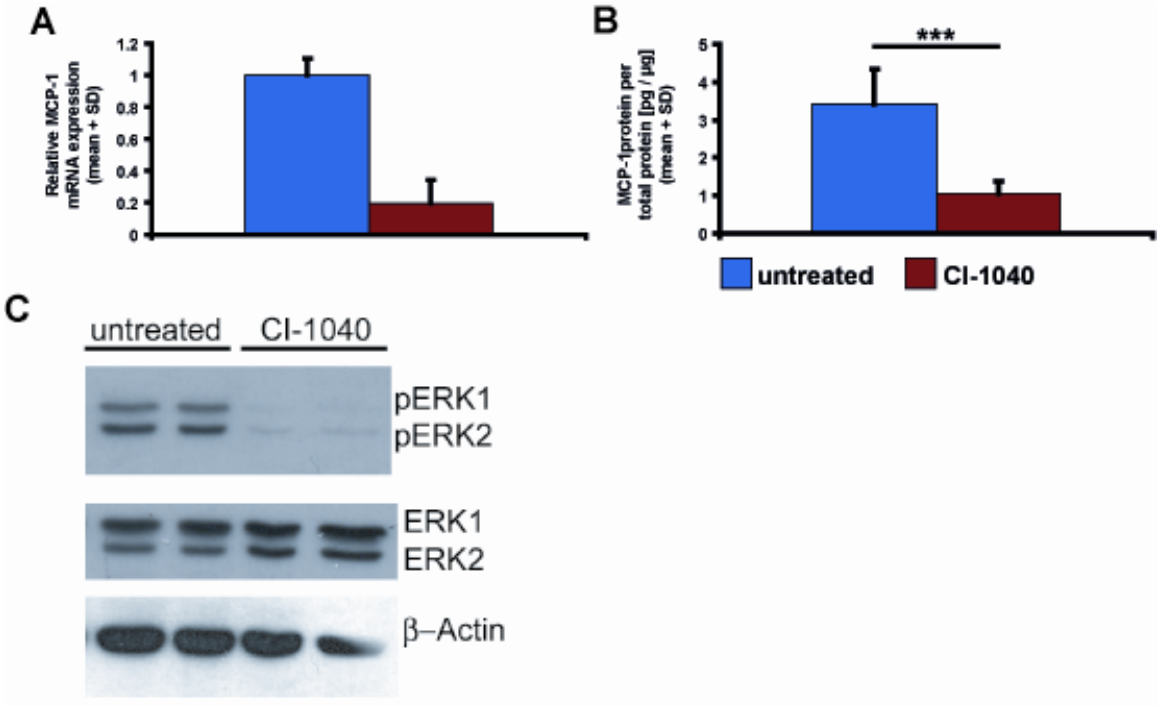

Figure 14: Inhibition of MEK1/2 in a Schwann cell line, Rn22, leads to a reduced phosphorylation of ERK1/2 and reduced expression of MCP-1 mRNA and protein.
Rn22 Schwann cell line exhibit expression of MCP-1 mRNA **(A)**, protein **(B)** and, additionally, phosphorylation of ERK1/2 **(C)**. Upon CI-1040 treatment decreased phosphorylation of ERK1/2 **(C)** is accompanied by decreased expression of MCP-1 mRNA **(A)** and protein **(B)**. Similar results were achieved by using supernatants. ***p < 0.001

In a next step the consequences of the inhibition of the MEK1/2-ERK1/2 signalling cascade were evaluated. For this purpose the MEK1/2-inhibitor CI-1040 which was gratefully provided by Pfizer (New York, USA) was used (Sebolt-Leopold et al., 1999; Sebolt-Leopold, 2000; Allen et al., 2003; Kramer et al., 2004). CI-1040 shows a high affinity and specificity for MEK1 and MEK2. After binding of CI-1040 to MEK1/2 kinases are still able to bind ERK1/2 but are no longer able to phosphorylate ERK1/2.

The addition of 10 mg/ml of CI-1040 to Schwannoma cell culture for three hours reduced the phosphorylation of ERK1/2 proteins and the expression of MCP-1 mRNA and protein significantly in one and the same culture (Figure 14). This effect of the MEK1/2-inhibitor CI-1040 was similar in all kinds of cultures which suggests that the Rn22 cell clone under the conditions used here showed an high activation of the observed MAPK-pathway, that the addition of CI-1040 had a striking effect on the activation of ERK1/2 and that the inhibition lead to a reduced expression of MCP-1 already after a short time period.

5.2.4 Systemic treatment of P0+/- mice with the MEK1/2-inhibitor CI-1040 results in reduced MCP-1 expression in peripheral nerves

To confirm a putative role of an activated MEK1/2-ERK1/2-cascade in the induction of MCP-1 in vivo in a model for inherited peripheral neuropathies, the P0+/- mice, systemic treatment with the MEK1/2 inhibitor CI-1040 was performed. P0+/+ mice and P0+/- mice were intraperitoneally treated with 100 mg per kg bodyweight of CI-1040 in DMSO for three weeks. Maximal 50 µl of DMSO was given due to side effects observed during an initial trial.

After three weeks of treatment peripheral nerves were dissected. Protein and total mRNA from sciatic nerves, femoral quadriceps and cutaneous saphenous nerves of single mice were purified from one and the same sample. Afterwards, phosphorylation of ERK1/2 proteins was evaluated by western blot and the amount of MCP-1 mRNA was measured by qRT-PCR using TaqMan assays. Due to the used protocol it was unfortunately not possible to test the amount of MCP-1 protein per total protein in peripheral nerves but it was possible to test in one and the same distinct nerve the phosphorylation status of ERK1/2 proteins as indicator for the inhibition of MEK1/2 by CI-1040 and the amount of MCP-1 mRNA by qRT-PCR.

Single P0+/- and P0+/+ mice were treated with (n = 10 / 7, respectively) or without (n = 8 / 6, respectively) 100 mg CI-1040 per bodyweight in 50 µl DMSO. Femoral quadriceps nerves of DMSO treated P0+/- mice showed increased phosphorylation of ERK1/2 in comparison to nerves from DMSO treated P0+/+ mice similar as described above (Figure 15A, B, Table 1). Femoral quadriceps nerve of CI-1040 treated P0+/+ mice showed instead a slight reduction of the phosphorylation of ERK1/2 in comparison to DMSO treated controls. Peripheral nerves of 1 out of 10 CI-1040 treated P0+/- mice showed no significant reduction in the phosphorylation of ERK1/2. But 9 out of 10 P0+/- mice treated with CI-1040 showed clear reduction in the phosphorylation of ERK1/2.

Table 1: ERK-activation and MCP-1 expression in P0+/- mice after 3weeks of treatment with CI-1040

Experiment	Nerve investigated	Reduced ERK1/2-activation*	Reduced MCP-1 mRNA*
1	Femoral quadriceps nerve, 3 months	3 / 3	3 / 3
2	Femoral quadriceps nerve, 3 months	4 / 4	4 / 4
3	Sciatic nerve, 6 months	2** / 3	2** / 3

*in comparison to sham-treated P0+/- mice

**a single animal not responding to CI-1040 treatment also failed to show MCP-1 mRNA reduction

Femoral quadriceps nerves of DMSO treated P0+/- mice showed as previously described additionally to enhanced phosphorylation of ERK1/2 and increased expression of MCP-1 mRNA in comparison to nerves from DMSO treated P0+/+ mice (Figure 15C). Although nerves from CI-1040 treated P0+/+ mice showed slightly diminished amount of phosphorylated ERK1/2 a clear reduction of MCP-1 mRNA expression is not obvious. Significantly, the reduction in the phosphorylation of ERK1/2 in peripheral nerves from CI-1040 treated P0+/- mice is accompanied by a decreased expression of MCP-1 mRNA (Figure 15C). Peripheral nerves of the single CI-1040 treated P0+/- mouse which does not show any reduction in the phosphorylation additionally shows no reduction in the expression of MCP-1 mRNA. This showed clearly that also *in vivo* the inhibition of the MEK1/2-ERK1/2 cascade can lead to reduced levels of MCP-1 mRNA expression.

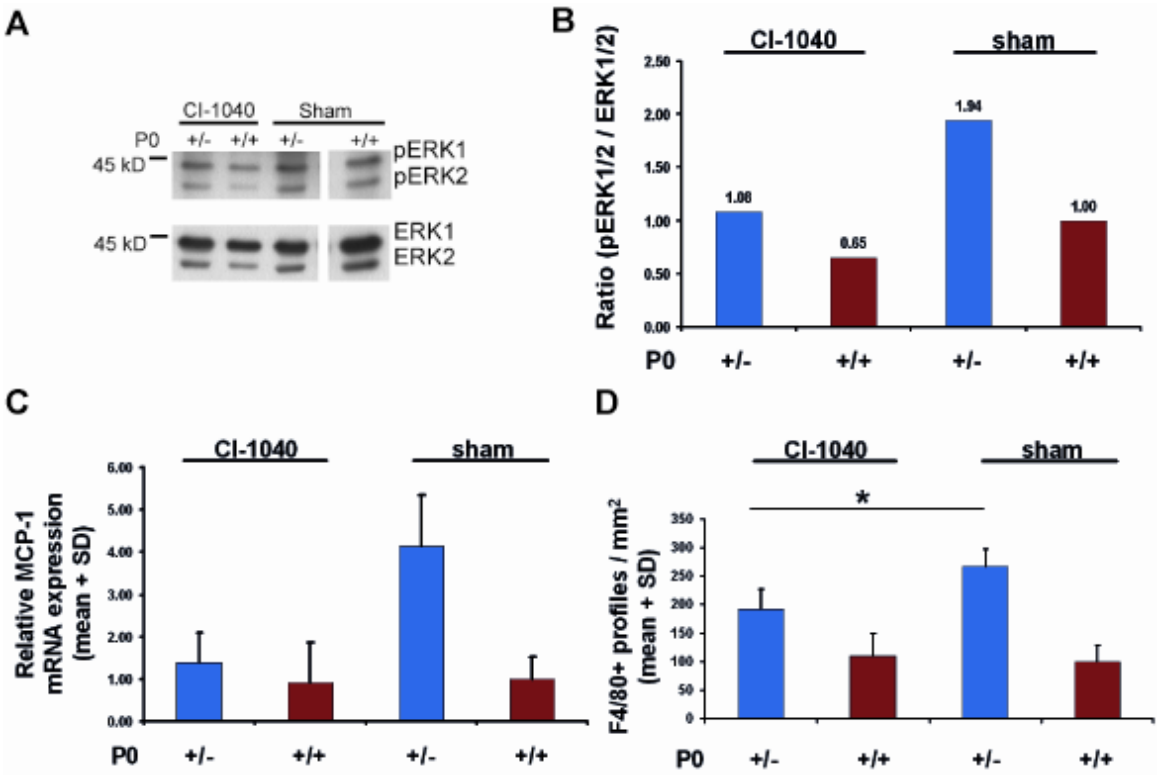

Figure 15: Treatment of P0+/+ and P0+/- mice with CI-1040 shows that reduction of ERK1/2 phosphorylation leads to a reduced expression of MCP-1 mRNA and to lowered numbers of macrophages in peripheral nerves.

(A) Similar to results obtained by cell culture the application of the MEK1/2-inhibitor leads to reduced phosphorylation of ERK1/2 in peripheral nerves of CI-1040 treated mice in comparison to sham-treated mice (femoral quadriceps nerve shown). **(B)** Densitometric analysis of **(A)** (values achieved with nerves from sham-treated P0+/+ mice set to one). **(C)** Reduction of phosphoERK1/2 leads to reduced expression of MCP-1 mRNA in one and the same nerve. **(D)** In lumbar ventral roots of same mice showing reduced ERK1/2 phosphorylation and MCP-1 mRNA expression in femoral quadriceps nerves reduced numbers of F4/80-postive cells in comparison to nerves from sham-treated P0+/- mice were quantified.

5.2.5 Inhibition of the MEK1/2-ERK1/2 cascade by CI-1040 leads to a significant reduction of macrophages in the endoneurium

In the previous sections it could be shown that MCP-1 plays a crucial role in the disease of P0+/- mice regarding the presence of macrophages in the endoneurium and demyelination and that the MEK1/2-ERK1/2 cascade is involved in regulation of MCP-1 expression. Therefore, peripheral nerves from mice used in the inhibition study were evaluated for an effect of CI-1040 treatment on the presence of macrophages in peripheral nerves.

Ventral spinal roots were investigated for the presence of F4/80-positive macrophages in CI-1040 and DMSO treated mice by immunohistochemistry. Figure 15D depicts the differences of macrophage numbers in lumbar ventral spinal roots per mm^2 which was necessary to avoid differences in size of spinal roots. Ventral spinal roots of P0+/+ mice treated either with CI-1040 or with DMSO alone showed similar numbers of F4/80-positive macrophages in the endoneurium (108.8 ± 40.6 and 100.2 ± 29.0 F4/80+ profiles/mm^2, respectively). DMSO treated P0+/- mice showed significant increased numbers of macrophages in ventral spinal roots (267.9 ± 29.8 F4/80+ profiles/mm^2) in comparison to roots of treated P0+/+ mice ($p = 0.007$ and $p = 0.002$ versus CI-1040 and DMSO treated P0+/+ mice, respectively). CI-1040 treated P0+/- mice showed in comparison to P0+/+ mice still an elevated quantity of F4/80-positive macrophages (192.2 ± 35.9 F4/80+ profiles/mm^2, $p = 0.056$ versus CI-1040 treated P0+/+; $p = 0.028$ versus DMSO treated P0+/+) in the endoneurium of ventral spinal roots. Nevertheless, in comparison to lumbar ventral roots of DMSO treated P0+/- mice significant decreased numbers of macrophages was obvious in ventral roots of CI-1040 treated P0+/- mice already after three weeks of treatment ($p = 0.050$).

These experiments showed that already after a short time of inhibition of the MEK1/2-ERK1/2 cascade by CI-1040 the reduction of MCP-1 expression resulted in a reduced population of macrophages into mutant peripheral nerves. Regarding the effects by a partial declined MCP-1 expression resulting in reduced numbers of macrophages as shown by P0/MCP-1 double mutant mice, the treatment with CI-1040 to reduce the expression of a pathologically relevant chemokine is conceptionally new and very promising in chronic demyelinating diseases of the peripheral nervous system.

6. Discussion

MCP-1, the monocyte chemoattractant protein-1, is a (C-C motif) chemokine ligand of around 15 kDa comprising one glycosylation site. It was first identified and described as chemoattractant agent for peripheral blood monocyte from culture medium conditioned by baboon aortic medial smooth muscle cells (Valente et al., 1988; Matsushima et al., 1989; Yoshimura et al., 1989a; Yoshimura et al., 1989b) and later on also shown as chemoattractive for various T-lymphocyte subsets (Allavena et al., 1994; Carr et al., 1994; Loetscher et al., 1996). Human and mouse MCP-1 show 68% identity (Yoshimura et al., 1989a) and can be expressed by monocytes, vascular endothelial cells, smooth muscle cells, glomerular mesangial cell, osteoblastic cells, gliomas and Schwann cells (Van Damme et al., 1992; Tofaris et al., 2002). The receptor for MCP-1 called CCR2 or CD192 is a seven transmembrane-spanning G-protein coupled receptor (Neote et al., 1993; Charo et al., 1994) which exists in two alternative splice variants, CCR2a and CCR2b (Sanders et al., 2000) leading upon ligand binding to activation of MEK1/2-ERK1/2 and STAT signalling cascades and to Ca^{2+} flux in case of CCR2a binding.

In the present study, we could show that MCP-1 is the first regulated cytokine in Schwann cells of P0+/- mice, a model for CMT1B, with a crucial role in the pathogenesis of chronic demyelinating disease. MCP-1 has an impact in recruiting macrophages into peripheral nerves of myelin mutants but also in healthy mice as it is constitutively expressed in peripheral nerves of P0+/+ mice. It further takes part in the course of pathology since peripheral nerves from P0+/-/MCP-1+/- mice show a striking amelioration of the primarily demyelinating disease in comparison to P0+/-/MCP-1+/+ mice. Peripheral nerves of P0+/-/MCP-1-/- mice instead exhibit an aggravation of axon pathology and the demyelinating phenotype in lumbar ventral roots. The differences of disease severity between P0+/-/MCP-1+/- and P0+/-/MCP-1-/- mice may be due to a putative compensatory regulation of cytokines like M-CSF.

MCP-1 expression is increased in peripheral nerves of P0+/- mice which is mainly due to expression in Schwann cells shown in the present study. Schwann cell expression of MCP-1 is induced by an activated MEK1/2-ERK1/2-signalling cascade which is temporary and spatial overlapping with MCP-1 expression in Schwann cells already before disease onset. *In vivo* inhibition of MEK1/2 leads to a reduction in ERK1/2 phosphorylation, a reduction of MCP-1 expression and a decrease in the total number of F4/80-positive macrophages suggesting therapeutical relevance of this pathway. In conclusion we partially describe a

molecular link between a Schwann cell based mutation and the induction of chemokine expression resulting in increased macrophage infiltration into peripheral nerves and a demyelinating disease in a model of human CMT1B.

6.1 Expression of MCP-1 in peripheral nerves

To identify molecules which might have impact on the onset of the demyelinating disease in peripheral nerves of P0+/- mice we focused on the expression of various cytokines in young mice. In P0+/- mice increased expression of MCP-1 mRNA and protein in comparison to P0+/+ mice could be shown in peripheral nerves already at the age of one, but also at the age of three, six and twelve months by qRT-PCR and ELISA, respectively.

An increased expression of MCP-1 was only found in nerves which will be or are affected from demyelinating disease, namely in femoral quadriceps nerves and sciatic nerves but not in cutaneous saphenous nerves. The lack of MCP-1 expression in cutaneous saphenous nerves accompanies the lack of increased numbers of macrophages and the absence of a demyelinating disease. Furthermore, elevated amounts of MCP-1 were already present in peripheral nervous tissue from P0+/- mice at one month of age, at a time point long before morphological visible onset of a demyelinating disease. This spatial and temporary distribution suggested a functional role of MCP-1 in the pathogenesis.

To further strengthen the hypothesis of a putative pathologically relevant function of MCP-1 we investigated the cellular source of MCP-1. In addition to astrocytes (Hayashi et al., 1995), macrophages (Lu et al, 1998) and endothelial cells (Sica et al., 1990) also neurons (Flugel et al., 2001) and Schwann cells (Tofaris et al., 2002) were described to be a source of MCP-1 in nervous tissue. *In-situ* hybridisation for MCP-1 mRNA in combination with immunohistochemistry against S100β was performed. The amount of MCP-1 mRNA detected was quite low as it is also shown by a very low expression in peripheral nerves of P0+/+ mice and an only 2.5 to 4 fold increase in nerves from one and three months old P0+/- mice by qRT-PCR. Therefore, MCP-1 mRNA was not detectable by *in-situ* hybridisation in peripheral nerves of P0+/+ mice at all which might be due to the sensitivity of the chosen technique.

In peripheral nerves of three months old P0+/- mice silver granules specific for MCP-1 mRNA were exclusively associated with S100β-positive structures and periaxonal collars, showing MCP-1 expression in Schwann cells. The amount of silver granules was increased in nerves

from six months old P0+/- mice in comparison to nerves from three months old P0+/- mice confirming results achieved by qRT-PCR. In peripheral nerves of six months old P0+/- mice additional granules were present in the endoneurium not associated with nerve fibers or S100β staining. Most probably these additional appearing cells at later time points are macrophages, which are present at higher frequency at this age, and fibroblasts which seem to play a distinct important function during pathogenesis (Antje Kroner, Bianca Kohl, unpublished results). Therefore, it is likely that MCP-1 expressed in Schwann cells is one of the first molecules crucial for the pathogenesis in P0+/- mice. Upon start of demyelination mediated by macrophages other cells might be secondarily activated and start to express MCP-1 and other proinflammatory cytokines.

Expression of MCP-1 by Schwann cells was already indicated by Tofaris and colleagues (Tofaris et al., 2002). Experiments with primary Schwann cells and the Schwannoma cell line Rn22 were used to evidence that MCP-1 secreted by Schwann cells can be chemoattractive for macrophages. Furthermore, the authors of this study propose a putative autocrine loop of IL-6 and LIF by Schwann cells inducing and enhancing expression of MCP-1 (Tofaris et al., 2002). This seems to be quite unlikely for peripheral nerves of one month old P0+/- mice as they do not display an increased expression of IL-6 or LIF mRNA relative to P0+/+ mice. At older ages, especially at six months increased IL-6 expression might influence MCP-1 expression in peripheral nerves of P0+/- mice. Moreover, induction of MCP-1 expression was shown to be mediated by TGFβ and IL-1β stimulation at least in human synovial cells during chronic inflammation (Yoshimura et al., 2006). Due to the fact that also for TGFβ and IL-1β no differences were found in peripheral nerves of one month old P0+/+ and P0+/- mice by qRT-PCR, initial MCP-1 expression seems not to be induced by other cytokines. Taking these results into account it is likely that the initial expression of MCP-1 at the age of one month, far earlier than any sign of pathology, is an intrinsic reaction of Schwann cells heterozygously deficient for P0.

MCP-1-/- mice were first described to evaluate the attraction of monocytes into inflamed tissue (Lu et al., 1998). Another striking result of this study was that peritoneal macrophages of MCP-1+/- mice express less MCP-1 under stimulation showing an intermediate expression relatively to stimulated peritoneal macrophages of MCP-1+/+ and MCP-1-/- mice. In the present study, the P0/MCP-1 double mutant mice were investigated regarding the expression of MCP-1 in peripheral nerves. In peripheral nerves of MCP-1-/- mice regardless of the P0 genotype MCP-1 was expectedly not detectable by ELISA. Peripheral nerves of P0+/-/MCP-1+/- mice showed reduced levels of MCP-1 protein similar to MCP-1 expression in peripheral nerves of P0+/+/MCP-1+/+ mice. Heterozygosity of *ccl2* leads also in peripheral

nerves to a reduced expression of MCP-1 protein but only under pathological conditions as P0+/+/MCP-1+/- do not exhibit a reduction of MCP-1 protein in comparison to P0+/+/MCP-1+/+ mice. P0+/+/MCP-1+/+ and P0+/+/MCP-1+/- mice showed by qRT-PCR and ELISA similar amounts of MCP-1 expression in peripheral nerves suggesting a level of constitutively expressed MCP-1 in naïve nerves. Therefore, it might be that under steady state condition without distinct induction of the MCP-1 gene, *ccl2*, heterozygous deficiency does not interfere with basal expression levels of MCP-1. Contrary after distinct induction of *ccl2* under pathological condition as likely in peripheral nerves of P0+/- mice a heterozygous MCP-1 deficiency might be observable as reduced amounts of MCP-1 protein expressed.

This might be even more relevant for chronic pathological conditions where no acute and strong regulation of gene transcription is visible as in peripheral nerves of P0+/- mice which show only a two to fourfold increase in MCP-1 mRNA. This view is strengthened by extensive promoter studies (Ueda et al., 1994; Freter et al., 1995; Takeshita et al., 1995; Ping et al., 1996; Martin et al., 1997; Bogdanov et al., 1998; Ping et al., 1999a; Ping et al., 1999b; Ping et al., 2000). These studies divide agents potent to stimulate MCP-1 expression into three different groups. Group I agents like cycloheximide mediate moderate expression probably due to opening of chromatin and usage of the proximal promoter region, whereas group II agents like TGFβ induce higher expression by usage of proximal promoter region and an enhancer region in the 3´ UTR. Highest expression was observed by parallel usage of the proximal and distal MCP-1 promoter region by agents of group III comprising TNF and IL-1. Due to the fact that at one month of age no other inflammatory cytokines were detectable in peripheral nerves of P0+/- so far and due to low level of MCP-1 expression we suggest the intrinsic regulation of *ccl2* by intracellular stress similar as induced by cycloheximide through the opening of chromatin and binding of already present and active transcription factors at the proximal region of the promoter. This view is even more strengthened due to the fact that under cycloheximide treatment an increased or sustained activation of ERK1/2 kinases is probable due to reduced expression of corresponding phosphatases (Bokemeyer et al., 1998) and that activated ERK1/2 kinases has been shown to activate histone acetyltransferases mediating the opening of chromatin for gene transcription (Swank and Sweatt, 2001; Koch et al., 2004)

6.2 Functional role of MCP-1 in peripheral nerves

The functional consequences of MCP-1 expression in peripheral nerves of P0+/- mice were evaluated by the generation of double mutant mice by crossbreeding P0+/- mice with MCP-1 deficient mice (Lu et al., 1998). In initial studies it could already been shown that MCP-1 deficient mice have a clear defect in the attraction of macrophages into inflamed tissue like into delayed-type hypersensitivity lesions (Lu et al., 1998). In peripheral nerves MCP-1 plays a key role in attraction of macrophages as shown in different kinds of lesion models. In tellurium-induced primary demyelination, nerve transection and nerve crush in rats the time course of MCP-1 expression in peripheral nerves is compatible with the recruitment of macrophages. Schwann cells were identified as the main source of MCP-1 in these studies (Toews et al., 1998; Taskinen and Roytta, 2000). Another study revealed an important function of MCP-1 expression in the regeneration of peripheral nerve injury (Perrin et al., 2005). After transection of mouse sciatic nerves MCP-1 and other cytokines are expressed distally of the injury. Infusion of functional blocking anti-MCP-1 antibodies into the region of the cut nerves resulted in a decrease in total and phagocytosing macrophages and an increase in intact myelin sheaths present in the transected nerves seven days after injury.

Therefore, cell numbers of immune cells inside the endoneurium of femoral quadriceps and cutaneous saphenous nerves of P0/MCP-1 mice were quantified. Previous studies using mouse models for CMT1 diseases as P0+/- and Cx32-/- mice and crossbreed of P0+/- and Cx32-/- mice with immune-deficient mutants like RAG-1 and M-CSF deficient mice always showed a correlation of the number of immune cells and disease severity (Schmid et al., 2000; Carenini et al., 2001; Kobsar et al., 2002; Kobsar et al., 2003; Kobsar et al., 2005; Kobsar et al., 2006; Ip et al., 2006). In case of P0/MCP-1 double mutant mice the situation appears different. At the age of six months no clear morphological differences in peripheral nerves of P0+/-/MCP-1+/+, P0+/-/MCP-1+/- and P0+/-/MCP-1-/- mice are visible although the amount of endoneurial F4/80-positive macrophages and CD8-positive T-lymphocytes is reduced in MCP-1 deficient P0+/- mice (P0+/-/MCP-1+/- and P0+/-/MCP-1-/-).

To better understand the pathogenesis in peripheral nerves of P0/MCP-1 mice we decided to firstly investigate the classical role of MCP-1 as a chemotactic agent. For this purpose P0/MCP-1 mice were irradiated at the age of three months and transplanted with GFP-positive bone marrow (Maurer et al., 2003; Schilling et al., 2005; Muller et al., 2007). P0+/+ and P0+/- mice deficient for MCP-1 show a clear reduction in the percentage of GFP-positive

macrophages after three months of bone marrow transplantation. This effect shows a clear role for MCP-1 as chemoattractant for macrophages into peripheral nerves. Nevertheless, the total number of endoneurial macrophages was similar to MCP-1 competent mice. This discrepancy can be explained by the increased presence of GFP-negative, long-term resident macrophages in the endoneurium. These GFP-negative macrophages could either result from an increased proliferation rate of macrophages in peripheral nerves of MCP-1 deficient mice which compensate the reduced infiltration of macrophages or from a longer inhabitation of GFP-negative macrophages. Unfortunately, the investigations about proliferation in peripheral nerves for example via BrdU pulse did not work out due to methodical problems which could not be resolved but are still ongoing. Therefore, a final answer to this open question cannot be given here. At least in the case of P0+/-/MCP-1-/- mice an increased proliferation of macrophages seems to be realistic due to an increased expression of M-CSF in comparison to MCP-1+/+ and MCP-1+/- myelin mutant mice.

Peripheral nerves of twelve months old P0+/-/MCP-1+/- and P0+/-/MCP-1-/- mice exhibit lower numbers of macrophages and T-lymphocytes in the endoneurium. Although reduced numbers of endoneurial macrophages in twelve months old P0+/-/MCP-1+/- mice lead to an amelioration of the disease the slightly and non-significant reduction of macrophage numbers in P0+/-/MCP-1-/- mice leads to an even more severe phenotype in lumbar ventral roots. Therefore we conclude that on the one side MCP-1 has an important role in the recruitment of macrophages into peripheral nerves and that reduction of MCP-1 leads to reduced demyelination and numbers of macrophages. On the other side that total deletion of MCP-1 in peripheral nerves is deteriorating the course of disease.

6.3 Reduction but not total deletion of MCP-1 ameliorates the genetically mediated demyelinating disease in peripheral nerves

Due to the worsening of disease by homozygously MCP-1 deficiency and amelioration of disease by heterozygously MCP-1 deficiency in lumbar ventral roots of P0+/- mice MCP-1 seems to have a dual role. Additionally to a significant reduction of macrophage numbers in peripheral nerves of twelve months old P0+/-/MCP-1+/- mice CD4 T-lymphocytes numbers increase. Although the total number of these T-lymphocytes is outnumbered by the number of macrophages and still smaller than CD8-positive T-lymphocytes a functional role can not be excluded. CD4-positive T-lymphocytes do have a regulatory and modifying role in cell-

mediated immunity. Due to the low number of CD4-positive T-lymphocytes in peripheral nerves it is, until now, not possible to investigate these cells more in detail but it shows that changes in MCP-1 dosage influence the cellular composition of endoneurium. To further elucidate a putative role of CD4-positive T-lymphocytes and, at first hand, to characterize the influence of different amounts of MCP-1 present in peripheral nerves of different genotypes on the expression of cytokines, we investigated the expression of pro- and anti-inflammatory cytokines by qRT-PCR. This approach was assumed to be the best way to evaluate differences in the immune response by dealing with low amounts both of available tissue and immune cell numbers.

Unfortunately, most of the cytokines investigated did not show a significant regulation which is most probably due to a dilution effect of few immune cells expressing immune relevant cytokines under five to tenfold more glial cells. Nevertheless, two distinct patterns of pro- and anti-inflammatory cytokine expression can be described. Expression of one of the most relevant cytokines in T-helper type II (Th2) immune response, namely IL-10 which has striking effects as inactivator of macrophages (Martinez et al., 2008) was slightly (< 2-fold) increased in P0+/-/MCP-1+/- mice. Complementary, pro-inflammatory cytokines like TNFα and IL-1β were primarily upregulated in the more affected peripheral nerves of P0+/-/MCP-1+/+ and P0+/-/MCP-1-/- mice. In case of the macrophage activating cytokine M-CSF it was possible to clearly show a significant upregulation in P0+/-/MCP-1-/- mice on mRNA and on protein level. Whether TNFα and M-CSF are mediators for macrophage activation or the products of activated macrophages is not distinguishable. However, due to the data it seems plausible that M-CSF is responsible for a higher macrophage activation and/or expansion of macrophages in the endoneurium in P0+/-/MCP-1-/- in comparison to P0+/-/MCP-1+/- (Muller et al., 2007). This is even more likely due to increased numbers of foamy macrophages detected in peripheral nerves of P0+/-/MCP-1-/- mice and reduced numbers of foamy macrophages observed in peripheral nerves of P0+/-/MCP-1+/-. Apart from this our data indicate that the expression of pro- and anti-inflammatory cytokines parallels the phenotype and the differences of the presence of CD4 T-lymphocytes with regard to the expression of MCP-1.

Another possible cause for differences in the severity of the demyelinating disease of P0+/-/MCP-1+/+, P0+/-/MCP-1+/- and P0+/-/MCP-1-/- mice might be the recruitment or generation of a different kind of macrophage subtype into peripheral nerves (Geissmann et al., 2003; Sunderkotter et al., 2004; Gordon and Taylor, 2005; Schlueter and Glasgow, 2006). Several different concepts of macrophage characterisation were followed up in the near past. Among these studies it was shown that CCR2-deficient mice generate a reduced

population of Ly6C^{hi}CD11b^{+} macrophages, also called inflammatory macrophages, in peripheral blood due to a reduced emigration of precursors out of the bone marrow (Serbina and Pamer, 2006). These inflammatory macrophages do show an increased response against pathogens, can express TNF, IL-12 and can also produce nitric oxide (Serbina et al., 2008). If one would suggest that deficiency of MCP-1 results in a similar phenotype as CCR2 deficiency MCP-1 heterozygous deficient mice showing reduced amounts of MCP-1 should show a slightly reduced number of Ly6C^{hi}CD11b^{+} macrophages in peripheral blood which can be recruited into peripheral nerves. This would not explain the amelioration of the disease in peripheral nerves of P0+/-/MCP-1+/- mice in comparison to P0+/-/MCP-1-/- mice. Therefore, it is not likely that the different results achieved by heterozygous and homozygous deficiency of MCP-1 is only a matter of MCP-1 dosage and decreased recruitment of one specific cell population.

Rather probable is the generation of different subtypes of macrophages in peripheral nerves of P0+/-/MCP-1+/+, P0+/-/MCP-1+/- and P0+/-/MCP-1-/- mice. By use of GFP-bone marrow chimeras we could show that on the one hand recruitment of macrophages represented by GFP-positive macrophages is diminished into peripheral nerves of MCP-1 homozygous deficient mice. This experiment revealed on the other hand an increased number of GFP-negative macrophages in nerves from MCP-1 deficient mice in comparison to P0+/+/MCP-1+/+ and P0+/-/MCP-1+/+ mice suggesting an extended retention time of macrophages or an increased generation of macrophages by proliferation. The increased expression of M-CSF found in P0+/-/MCP-1-/- would favour an increased proliferation of GFP-negative macrophages inside peripheral nerves. This is even strengthened by previous findings showing that M-CSF is important for “activation, in situ increase and myelin phagocytosis” (Muller et al., 2007) of macrophages and by an increased amount of TNFα mRNA and higher numbers of foamy macrophages found in this study in peripheral nerves of P0+/-/MCP-1-/- mice. Further studies identifying the cellular source of M-CSF expression and evaluating the effect of M-CSF on macrophage activation, proliferation and differentiation in situ are therefore necessary to clarify the events in peripheral nerves of P0/MCP-1 double mutant mice.

The aggravated diseased phenotype of P0+/-/MCP-1-/- mice might be additionally due to a non-immunological function of MCP-1 in peripheral nerves. This hypothesis is strengthened by the findings that MCP-1 is expressed in naïve primary cultured rat Schwann cells (Karanth et al., 2006) and healthy mouse peripheral nerves where it mediates the recruitment of macrophages into the endoneurium shown by the GFP-bone marrow chimeras in this study. Furthermore, the expression of MCP-1 in Schwann cells can be induced by several different

stimuli (Taskinen and Roytta, 2000; Tofaris et al., 2002; Tanaka et al., 2004; Perrin et al., 2005; Karanth et al., 2006; Zhang and De Koninck, 2006) and may therefore play a central role in nerve de- and regeneration. Additionally, the total absence of MCP-1 in peripheral nerves of P0+/- mice reveals a putative neurotrophic role of this chemokine shown by increased axonopathic changes in P0+/-/MCP-1-/-.

6.4 Regulation of MCP-1 expression in peripheral nerves of P0+/- mice

Most of current therapeutic concepts in treating peripheral but also central nervous system disorders mediated by the immune system like severe forms of Guillain-Barré-Syndrom and multiple sclerosis are dealing with general immunosuppressive or immunomodulatory agents. Therefore, one aim of these studies was to identify and characterize a molecular target of immune-mediated peripheral nerve disorders using a mouse model for CMT1B. Specific inhibitors of signalling kinases which are currently promising therapeutic agents already used in clinical trials were considered to be tested in peripheral nerve disorders.

Extensive evaluation of the phosphorylation status of several specific kinases has been performed using phosphorylation-specific antibodies against activation sites of signalling kinases. These investigations were concentrated on kinases which were already proven to be involved in the activation of the MCP-1 gene, *ccl2*, using peripheral nerves from mice of one, three, six and twelve months of age (Sheng et al., 2005; Waetzig et al., 2005; Yoo et al., 2005; Ip et al., 2006; Venkatesan et al., 2006).

These studies were started with three and six months old mice which reveal strong and sustained phosphorylation of ERK1 and ERK2 in femoral quadriceps and sciatic nerves of P0+/- mice. The putative pathological role of activated ERK1/2 kinases was confirmed using cutaneous saphenous nerve lysates. These nerves which are not affected by demyelination show no different phosphorylation of ERK1/2 in P0+/- in comparison to P0+/+ mice. Further analyses revealed that also the direct upstream components of the MEK1/2-ERK1/2 cascade, namely MEK1 and MEK2, are phosphorylated in a higher fashion in peripheral nerves of P0+/- mice affected by demyelinating disease than in nerves from P0+/+. In this group of mice only phosphorylation of STAT1α in peripheral nerves of six months old and PKCα in three and six months old P0+/- mice was differently phosphorylated from age-matched P0+/+ mice.

Subsequently, one month old mice were investigated showing no sign of pathology despite expression of MCP-1. Phosphorylation of ERK1/2 proteins was elevated in femoral quadriceps and sciatic nerves of P0+/- mice in contrast to P0+/+ mice. Due to reasons of sensitivity it was not able to investigate MEK1/2 in peripheral nerves of one month old single mice but in two months old mice increased MEK1/2 and ERK1/2 phosphorylation could be also shown. From these analyses only the MEK1/2-ERK1/2 cascade overlaps temporary with the expression of MCP-1. This leads to the hypothesis that this activated signalling cascade in mutants may have pathological impact on induction of MCP-1 expression long before disease onset.

The primary defect in P0+/- mice is carried by Schwann cells which do not solely express P0 in mice (Visan, 2003) but do obviously suffer from heterozygously deletion. Two molecular mechanisms may lead from reduced P0 protein dosage to a chronic progressive peripheral neuropathy starting between infancy and adulthood. On the one side Schwann cells increasing the amount of myelin until adulthood due to growing axons may start to suffer from a low amount of myelin protein during growth and may activate a kind of stress response leading in the following to ERK1/2 activation. Another possibility might be a direct link between P0 and the signalling compartment of Schwann cells. P0 carries a target site for PKCα (Xu et al., 2001; Gaboreanu et al., 2007) which seems to be important for the adhesive function of P0 at least *in vitro*. However, Schwann cells might respond to a myelin-related mutation due to the intensive expression of myelin proteins and the tight relation between axon-glia interrelation which is at least partly mediated by intact myelin sheaths and therefore based on functioning myelin protein expression.

So far, the MEK1/2-ERK1/2 signalling cascade was mainly supposed to take part in trophic and proliferating cellular events whereas other MAPK-signalling pathways like p38 and JNK are more involved in stress responses (Roux and Blenis, 2004; Aouadi et al., 2006; Gerits et al., 2007). This was impressingly shown in case of Nerve Growth factor (NGF)-signalling in peripheral nerves (Johanson et al., 1995; Averill et al., 2001; Middlemas et al., 2003) leading to Trk-receptor internalization in axons and axonal transport of activated signalling kinases towards the cell body. Specific axonal staining for phosphorylated ERK1/2 proteins in single nerve fiber preparations but also cross sections of peripheral nerves of P0+/- and P0+/+ mice are not differing suggesting that NGF-stimulated ERK1/2 activation is not modulated by P0 heterozygosity and therefore not influenced by or influencing the signalling in Schwann cells. During the last years it came out that the MEK1/2-ERK1/2 cascade has an implication in cell differentiation and immunological response. Immunohistochemical analysis revealed that phosphorylated ERK1/2 proteins are present in Schwann cell nuclei at time points, one to

three months of age, where no increased Schwann cell proliferation and increased Schwann cell numbers are present or before demyelination and macrophage influx starts but MCP-1 expression occurs. Therefore, the temporary and spatial correlation of ERK1/2 phosphorylation and MCP-1 expression inside Schwann cells before onset of disease is specific for pathological affected peripheral nerves of P0+/- mice and likely interrelated inside of affected Schwann cells.

The activation of the MEK1/2-ERK1/2 signalling cascade does not necessarily lead to a proliferation of Schwann cells. Indeed, at the age of six months increased numbers of cells are present in femoral quadriceps nerves from P0+/- mice in comparison to P0+/+ mice which might reflect cell proliferation based upon an activated MEK1/2-ERK1/2 signalling cascade. This is not true in peripheral nerves of one and three months old P0+/- mice despite MEK1/2-ERK1/2 activation. The increased number of cells in affected peripheral nerves of six months old P0+/- mice which is partially due to macrophage immigration and most probably macrophage proliferation is also due to Schwann cell dedifferentiation and proliferation as it occurs during peripheral nerve degeneration and regeneration (Scherer and Salzer, 1996). This results in the occurrence of supernumerary Schwann cells and onion bulbs as it can be seen in peripheral nerves of six months old P0+/- mice. Similar results were achieved recently showing that sustained activation of ERK1/2 is responsible for dedifferentiation of Schwann cells (Harrisingh et al., 2004) or can suppress the differentiation of Schwann cells (Ogata et al., 2004). Therefore, it is likely to assume that the activation of the MEK1/2-ERK1/2 signalling cascade in affected peripheral nerves of P0+/- mice is part of a dedifferentiation program of Schwann cells leading at the end to a regeneration of peripheral nerves. This dedifferentiation program might include the expression of MCP-1 by Schwann cells one step ahead of debonding of Schwann cells from axons to drive macrophage activation, immigration and probably tissue remodelling by macrophages.

6.5 *In vivo* inhibition of MEK1/2 reduces the expression of MCP-1

A specific MEK1/2-inhibitor, CI-1040, was used *in vivo* to test if there is a direct link between MCP-1 mRNA expression and ERK1/2 phosphorylation. The inhibitor was daily injected intraperitoneally into mice for three weeks. CI-1040 is hydrophobic and so necessarily solubilized in DMSO which impeded the treatment. Due to the toxicity of DMSO and spontaneous death after application of higher amounts of DMSO it was further necessary to reduce the injected volume to a minimum. To control side effects of the solvent sham-treated

mice were injected with the same volume of DMSO. A minority of mice was loosing weight during the study and were therefore excluded from the study.

After three weeks of treatment peripheral nerves of treated mice were dissected and tested for the amount of phosphorylated ERK1/2 proteins and MCP-1 mRNA. In a first approach, pooled samples were used consisting of femoral quadriceps, cutaneous saphenous or sciatic nerves of two to three mice. P0+/+ mice treated with CI-1040 or sham-treated P0+/+ and P0+/- mice showed no obvious differences in comparison to non-treated mice in regard of MCP-1 expression or phosphorylation of ERK1/2 in peripheral nerves. Femoral quadriceps and sciatic nerves of CI-1040 treated P0+/- mice showed a clear reduction in ERK1/2 phosphorylation in comparison to sham-treated P0+/- mice. The same samples revealed also reduced levels of MCP-1 mRNA expression showing a clear impact of phosphorylation of ERK1/2 on the expression of MCP-1 mRNA.

In another experiment using 50 mg CI-1040 per kg bodyweight some samples from inhibitor-treated P0+/- mice showed no reduction of ERK1/2 activation and MCP-1 mRNA amount in comparison to sham-treated mice. Due to the reduced dosage of CI-1040 used in this approach it might be that CI-1040 was not able to surmount obstacles like the blood-nerve-barrier in increased numbers of mice.

Three experiments using a dosage of 100 mg CI-1040 per kg bodyweight and producing samples from single mice's nerves showed a convincing and reproducible inhibition of ERK1/2 phosphorylation in peripheral nerves of CI-1040 treated P0+/- mice in comparison to sham-treated mice. Out of ten mice nine CI-1040 treated mice exhibit a clear reduction of phosphorylated ERK1/2 proteins in peripheral nerves. This inhibition was paralleled by a reduction of MCP-1 mRNA expression in one and the same sample. Only in one investigated mouse it was not possible to show reduced phosphorylation of ERK1/2 proteins without reduction of MCP-1 mRNA expression in sciatic nerve. The majority of CI-1040 treated mice showed the expected effect of reduced phosphorylation of ERK1/2 on MCP-1 mRNA expression suggesting that in pathological altered peripheral nerves of P0+/- mice an activated MEK1/2-ERK1/2 cascade is necessary for MCP-1 expression. Further experiments have to be done to unveil an direct effect of phosphorylated ERK1/2 proteins on transcription factor activation or histone modification in mutant Schwann cells in nerves from P0+/- mice.

Finally, effects of reduced MCP-1 mRNA amounts in ventral spinal roots of CI-1040 treated P0+/- mice on the presence of macrophages were investigated to show a clinical relevance of this therapeutic strategy. We assumed that also after a short time inhibitor treatment there

might already be an effect visible on the cellular composition of peripheral nerves. The reason for choosing ventral spinal roots and not femoral quadriceps nerves was the availability of tissue. Due to the previous experiments about the differences in disease course of femoral quadriceps and cutaneous saphenous nerves which are both branches of the femoral nerve the molecular effect of CI-1040 was investigated in these nerves which leads to the necessity to use all of the dissected tissue. Therefore, ventral spinal roots were used which behave similar to quadriceps nerve regarding macrophage influx, disease onset, MCP-1 expression and activation of MEK1/2-ERK1/2 cascade. Additionally, most significant differences in morphology in P0/MCP-1 mice were seen in ventral spinal roots suggesting that minor differences might be easier visible there. By this it could be shown that in P0+/- mice showing reduced levels of ERK1/2 phosphorylation and MCP-1 mRNA expression in femoral quadriceps nerves by administration of the MEK1/2-inhibitor CI-1040 for three weeks leads to reduced numbers of F4/80-positive macrophages in ventral spinal roots. A functional role of the MEK1/2-inhibition on the survival of macrophages could not be investigated and cannot be ruled out. However, the reduced phosphorylation of ERK1/2 leads to reduced expression of MCP-1 mRNA and as hypothesized also to reduced numbers of macrophages in peripheral nerves of CI-1040 treated P0+/- mice in comparison to sham-treated mice.

In summary, we could newly identify some of the molecular events in a mouse model for CMT1B, the P0+/- mice, in the early phase of pathogenesis. MCP-1 was characterized as an agent with a striking function in diseased but also in healthy nerves by recruiting macrophages into the endoneurium. Deletion of MCP-1 by crossbreeding MCP-1 deficient and P0 deficient mice showed that heterozygously but not homozygously MCP-1 deficiency leads to an amelioration of the demyelinating disease. The morphology revealed in lumbar ventral roots of homozygous MCP-1 deficient P0+/- mice strongly suggests an additional, neuroprotective function of MCP-1 in peripheral nerves. Furthermore, the MEK1/2-ERK1/2 cascade is linked to the induction of MCP-1 mRNA expression in diseased nerves of P0+/- mice and can be targeted for therapeutic approaches as shown by animal experiments using a specific MEK1/2 inhibitor. This might therefore for the first time represent a direct link between a Schwann cell based mutation in a CMT1B mouse model and a specific putative therapeutic strategy by *in vivo* application of specific inhibitors for underlying signalling cascades.

7. Appendices

7.1. Appendix 1: Technical equipment

BioPhotometer 6131 (Eppendorf, Hamburg, Germany);

Centrifuges: Biofuge 15R and Biofuge Pico (Heraeus, Hanau, Germany),
Centrifuge 5810R and Centrifuge 5415C (Eppendorf, Hamburg, Germany),
Rotofix 32 (Hettich Zentrifugen, Tuttlingen, Germany);

ELISA reader Multiskan EX (Labsystems, Frankfurt, Germany);

Gel chamber, horizontal (PeqLab, Erlangen, Germany);

Dry Block Thermostate TDB-120 (Hartenstein, Würzburg, Germany);

Incubators HeraCell150 (Heraeus, Hanau, Germany);

Cryostat: CM 1900 and CM 3050S (Leica, Wetzlar, Germany);

Microscopes: CX31, BH2 and CKX41 (Olympus, Hamburg, Germany),
Axioplan/Axiophot 2 and Axiostar plus (Zeiss, Göttingen, Germany),
Leo 906 E electron microscope (Zeiss, Oberkochen, Germany) with an attached SlowScan CCD camera (ProScan, Lagerlechfeld, Germany),
TCS SP2 mounted to a DM RE-7 SDK microscope (Leica Microsystems, Wetzlar, Germany);

Pipettes: Abimed (Berlin, Germany),
Eppendorf (Hamburg, Germany),
Gilson (Bad Camberg, Germany);

Thermocycler: Mastercycler gradient (Eppendorf, Hamburg, Germany);
Primus96 advanced (Peqlab, Erlangen, Germany)

Cell culture bottles (Sarstedt, Nümbrecht, Germany);

Object slides superfrost (Langenbrinck, Teningen, Germany);

PapPen (SCI, Munich, Germany);

PCR tubes (Sarstedt, Nümbrecht, Germany);

Reaction tubes 0.5ml, 1.5ml, 2ml, 15ml, 50ml (Sarstedt, Nümbrecht, Germany);

Vertical gel chamber Mini Protean and Mini Trans Blot (Bio-Rad, München, Germany);

Sonication device: Sonoplus HD60 (Bandelin electronic, Berlin, Germany);

Speed Vac: Vacobox (KNF Neuberger, Freiburg i. Br., Germany)
Unicryo MC 2L -60.0C (UniEquip, Planegg, Germany)
mounted to Univapo 100 H (UniEquip, Planegg, Germany);

UV Crosslinker 1800, (Stratagene, La Jolla, CA 92037; USA).

7.2. Appendix 2: Cell culture media and solutions

- Medium for NIH 3T3 and HeLa cells:

10 – 20% FCS
1% Glutamate
1% Penicillin/Streptomycin
in DMEM

- Medium for Rn22 cells:

10 % FCS
in DMEM, supplemented with Glutamate

- Freeze medium:

20 % (v/v) FCS
20 % DMSO
in DMEM

-**Trypsin** (Invitrogen, Karlsruhe, Germany)
- **Glutamate** (Invitrogen, Karlsruhe, Germany)
- **Penicillin/Streptomycin** (Invitrogen, Karlsruhe, Germany)
- **FCS** (Biochrom, Berlin, Germany)

7.3. Appendix 3: Buffers and solutions

- **Anaesthetic:**

- 0.6 % Ketanest
- 0.08 % Rompun
- 8.3 % NaCl

- **RIPA lysis buffer:**

- 25 mM Tris pH 8
- 10 mM Hepes pH 4.4
- 150mM NaCl
- 5mM $MgCl_2$
- 145 mM KCl
- 0.4 % EDTA
- 0.1 % SDS
- 1% Nonidet P40
- 10 % Glycerol

- **1x PBS:**

- 137 mM NaCl
- 2.7 mM KCl
- 1.5 mM KH_2PO_4
- 8.1 mM Na_2HPO_4

- **1x PBST:**

- 0.1 % Tween 20
- in 1x PBS

- **TBE:**

- 89 mM Tris
- 89 mM Borate
- 2 mM EDTA
- pH 8.0

- **DABCO:**

- 25 % 1x PBS
- 75 % Glycerol
- 25 mg/ml 1,4-diazabicyclo[2.2.2]octane

- **4x Separating gel buffer:**

- 1.5 M Tris
- 0.4 % SDS
- 0.4 % TEMED
- pH 8.8

- **4x Stacking gel buffer:**

- 0.5 M Tris
- 0.4 % SDS
- 0.4 % TEMED
- pH 6.8

- **10x SDS PAGE buffer:**

- 0.25 M Tris
- 1.92 M Glycine
- 1 % SDS

- **10x Transfer buffer:**

- 0.25 M Tris
- 1.92 M Glycine

- **1x Transfer buffer:**

- 20% MetOH
- in 1x Transfer buffer

- **Stripping-buffer:**

- 0.2 M Glycine
- 0.1 % SDS
- 20 mM Dithiotreitol
- 1 % Tween 20
- pH 2.1

- **Spurr`s medium:**

- 10g ERL 4206
(3,4-Epoxycyclohexylmethyl-3,4-epoxycyclohexylcyclocarboxylate)
6 g DER 736
26 g NSA (Nonenylsuccinicanhydride)
0.4 g DMAE (Dimethylaminoethanol)

7.4. Appendix 4: Primer sequences

Sequences of used primers	
Primer	**Sequence**
S 1295	5´-TCA GTT CCT TGT CCC CCG CTC TC-3´
AS 1772	5´-ACT TGT CTC TTC TGG GTA ATC AA-3´
AS 1606	5´-GGC TGC AGG GTC GCT CGG TGT TC-3´
MCP-1 F	5´-GGAGCATCCACGTGTTGGC-3´
MCP-1 R	5´-ACAGCTTCTTTGGGACACC-3´
IMRO 60	5´-AGGATCTCGTCGTGACCCATG-3´

7.5. Appendix 5: *In-situ* target sequence

Genbank accession no.: M19681, 1892-2062, 181bp fragment,
tcggaaccaa atgagatcag aacctacaac tttatttaaa actgcatctg ccctaaggtc ttcagcacct ttgaatgtga agttgacccg taaatctgaa gctaatgcat ccactacctt ttccacaacc acctcaagca cttctgtagg agtgaccagt gtgacagtga a

7.6. Appendix 6: Antibodies used in western blot analyses

Primary and secondary antibodies for western blot analyses				
Primary antibody	**Company**	**Clone**	**Concentration/ Dilution**	**Product number**
Rabbit-anti-actin Ab	Sigma Aldrich	poly	1 : 500	A 2066
Rabbt-anti-p-Akt (Ser473) mAb	Cell Signaling	193H12	1 : 1000	4058
Rabbit-anti-Akt2 mAb	Cell Signaling	5B5	1 : 1000	2964
Mouse-anti-p-ERK1/2 (Tyr204) mAb	Santa Cruz	E4	0.2 µg/ml	SC-7383
Rabbit-anti-ERK1 Ab	Santa Cruz	poly, K-23	0.02 µg/ml	SC-94
Rabbit-anti-p-IκBα (Ser32) Ab	Cell Signaling	14D4	1 : 200	9241
Rabbit-anti-IκBα Ab	Cell Signaling	poly	1 : 200	9242
Mouse-anti-p-JNK mAb	Santa Cruz	G-7	0.2 µg / ml	SC-6254
Rabbit-anti-JNK1 Ab	Santa Cruz	poly, FL	0.2 µg / ml	SC-571

Primary antibody	Company	Clone	Concentration/ Dilution	Product number
Rabbit-anti-p-MEK1/2 (Ser218/222) Ab	Chemicon	poly	1 : 1000	AB3810
Rabbit-anti-MEK1/2 Ab	Cell Signaling	poly	1 : 1000	9122
Rabbit-anti-p65 Ab	Santa Cruz	poly, H-286	2 µg / ml	SC-7151
Rabbit-anti-p-p38 (Thr180/Tyr182) Ab	Chemicon	poly	1 : 1000	AB3828
Rabbit-anti-p38 Ab	Chemicon	poly	1 : 1000	AB3188
Rabbit-anti-PI 3-Kinase p85 (N-SH2-domain) Ab	Upstate	poly	2 µg / ml	06-496
Rabbit-anti-p-PKCα (Ser657) Ab	Santa Cruz	poly	0.2 µg / ml	SC-12356R
Rabbit-anti-PKCα Ab	Santa Cruz	H-300	0.2 µg / ml	SC-10800
Rabbit-anti-p-STAT1 (Tyr701) Ab	Chemicon	poly	10 µg / ml	AB3892
Rabbit-anti-STAT1α Ab	Chemicon	poly	2 µg / ml	AB16951
Rabbit-anti-STAT3 Ab	Chemicon	poly	5 mg / ml	AB3162
Mouse-anti-p-tyrosine mAb	Cell Signaling	-	1 : 2000	9411

Secondary antibody	Company	Clone	Concentration/ Dilution	Product number
Sheep-anti-mouse-IgG HRP conjugated Ab	Chemicon	poly	1 : 4000	AP300P
Sheep-anti-rabbit-Ig HRP conjugated Ab	Chemicon	poly	1 : 2000	AP322P

7.7. Appendix 7: Antibodies used in immunohistochemistry

Antibodies used in immunohistochemistry				
Primary antibody	**Company**	**Clone**	**Concentration/ Dilution**	**Fixation/ Additives**
Sheep anti-bovine S100β	Biodesign	M55202S	1/500	- / -
Rabbit anti-S100	DAKO	Z0311	1/400	- / -
Rat anti-mouse F4/80	Serotec	MCA497	3 µg/ml	- / -
Rat anti-mouse CD8	Chemicon	CBL1325 / 2F7	5 µg/ml	Acetone, 10 minutes -20°C / -
Rat anti-mouse CD4	Serotec	MCA1767 / YTS191.1	1µg/ml	Acetone, 10 minutes -20°C / -
Rat anti-mouse CD68	Serotec	MCA1957 / FA-11	2µg/ml	- / -
Rabbit anti-mouse phosphoERK1/2	Chemicon	AB3826	1:100	- / 0.3% Triton
Rabbit anti-ERK1	Santa Cruz	Poly, K-23	2µg/ml	- / 0.3% Triton

Secondary antibody	**Company**	**Clone**	**Concentration/ Dilution**
FITC-conjugated Donkey-anti-sheep IgG (H&L)	Rockland	613-702-168	10µg/ml
Cy3-conjugated Goat-anti-rabbit IgG (H&L)	Dianova	111-165-144	1/300
Biotinylated Rabbit-anti-rat IgG (H&L)	Vector labs	BA4001	1/300

8. References

Allavena P, Bianchi G, Zhou D, van Damme J, Jilek P, Sozzani S, Mantovani A (1994) Induction of natural killer cell migration by monocyte chemotactic protein-1, -2 and -3. Eur J Immunol 24:3233-3236.

Allen LF, Sebolt-Leopold J, Meyer MB (2003) CI-1040 (PD184352), a targeted signal transduction inhibitor of MEK (MAPKK). Semin Oncol 30:105-116.

Aouadi M, Binetruy B, Caron L, Le Marchand-Brustel Y, Bost F (2006) Role of MAPKs in development and differentiation: lessons from knockout mice. Biochimie 88:1091-1098.

Asensio VC, Kincaid C, Campbell IL (1999) Chemokines and the inflammatory response to viral infection in the central nervous system with a focus on lymphocytic choriomeningitis virus. J Neurovirol 5:65-75.

Averill S, Delcroix JD, Michael GJ, Tomlinson DR, Fernyhough P, Priestley JV (2001) Nerve growth factor modulates the activation status and fast axonal transport of ERK 1/2 in adult nociceptive neurones. Mol Cell Neurosci 18:183-196.

Benninger Y, Thurnherr T, Pereira JA, Krause S, Wu X, Chrostek-Grashoff A, Herzog D, Nave KA, Franklin RJ, Meijer D, Brakebusch C, Suter U, Relvas JB (2007) Essential and distinct roles for cdc42 and rac1 in the regulation of Schwann cell biology during peripheral nervous system development. J Cell Biol 177:1051-1061.

Blakemore WF (1974) Pattern of remyelination in the CNS. Nature 249:577-578.

Boekhoudt GH, Guo Z, Beresford GW, Boss JM (2003) Communication between NF-kappa B and Sp1 controls histone acetylation within the proximal promoter of the monocyte chemoattractant protein 1 gene. J Immunol 170:4139-4147.

Bogdanov VY, Poon M, Taubman MB (1998) Platelet-derived growth factor-specific regulation of the JE promoter in rat aortic smooth muscle cells. J Biol Chem 273:24932-24938.

Bokemeyer D, Lindemann M, Kramer HJ (1998) Regulation of mitogen-activated protein kinase phosphatase-1 in vascular smooth muscle cells. Hypertension 32:661-667.

Braunersreuther V, Mach F, Steffens S (2007) The specific role of chemokines in atherosclerosis. Thromb Haemost 97:714-721.

Britsch S, Li L, Kirchhoff S, Theuring F, Brinkmann V, Birchmeier C, Riethmacher D (1998) The ErbB2 and ErbB3 receptors and their ligand, neuregulin-1, are essential for development of the sympathetic nervous system. In, pp 1825-1836.

Campbell IL, Hobbs MV, Kemper P, Oldstone MB (1994) Cerebral expression of multiple cytokine genes in mice with lymphocytic choriomeningitis. J Immunol 152:716-723.

Carenini S, Maurer M, Werner A, Blazyca H, Toyka KV, Schmid CD, Raivich G, Martini R (2001) The role of macrophages in demyelinating peripheral nervous system of mice heterozygously deficient in p0. Journal of Cell Biology 152:301-308.

Carpenter EM, Hollyday M (1992) The location and distribution of neural crest-derived Schwann cells in developing peripheral nerves in the chick forelimb. Dev Biol 150:144-159.

Carr MW, Roth SJ, Luther E, Rose SS, Springer TA (1994) Monocyte chemoattractant protein 1 acts as a T-lymphocyte chemoattractant. Proc Natl Acad Sci U S A 91:3652-3656.

Cecchini MG, Dominguez MG, Mocci S, Wetterwald A, Felix R, Fleisch H, Chisholm O, Hofstetter W, Pollard JW, Stanley ER (1994) Role of colony stimulating factor-1 in the establishment and regulation of tissue macrophages during postnatal development of the mouse. Development 120:1357-1372.

Charo IF, Myers SJ, Herman A, Franci C, Connolly AJ, Coughlin SR (1994) Molecular cloning and functional expression of two monocyte chemoattractant protein 1 receptors reveals alternative splicing of the carboxyl-terminal tails. Proc Natl Acad Sci U S A 91:2752-2756.

Chitu V, Stanley ER (2006) Colony-stimulating factor-1 in immunity and inflammation. Curr Opin Immunol 18:39-48.

Chomczynski P, Sacchi N (1987) Single-step method of RNA isolation by acid guanidinium thiocyanate-phenol-chloroform extraction. Anal Biochem 162:156-159.

Cramer T, Juttner S, Plath T, Mergler S, Seufferlein T, Wang TC, Merchant J, Hocker M (2008) Gastrin transactivates the chromogranin A gene through MEK-1/ERK- and PKC-dependent phosphorylation of Sp1 and CREB. Cell Signal 20:60-72.

Dawson J, Miltz W, Mir AK, Wiessner C (2003) Targeting monocyte chemoattractant protein-1 signalling in disease. Expert Opin Ther Targets 7:35-48.

Dong Z, Brennan A, Liu N, Yarden Y, Lefkowitz G, Mirsky R, Jessen KR (1995) Neu differentiation factor is a neuron-glia signal and regulates survival, proliferation, and maturation of rat Schwann cell precursors. Neuron 15:585-596.

Doya H, Ohtori S, Takahashi K, Aoki Y, Ino H, Takahashi Y, Moriya H, Yamashita T (2005) Extracellular signal-regulated kinase mitogen-activated protein kinase activation in the dorsal root ganglion (DRG) and spinal cord after DRG injury in rats. Spine 30:2252-2256.

Feldmann M, Brennan FM, Williams RO, Elliott MJ, Maini RN (1995) Cytokine expression and networks in rheumatoid arthritis: rationale for anti-TNF alpha antibody therapy and its mechanism of action. J Inflamm 47:90-96.

Feltri ML, Graus Porta D, Previtali SC, Nodari A, Migliavacca B, Cassetti A, Littlewood-Evans A, Reichardt LF, Messing A, Quattrini A, Mueller U, Wrabetz L (2002) Conditional disruption of beta 1 integrin in Schwann cells impedes interactions with axons. J Cell Biol 156:199-209.

Flugel A, Hager G, Horvat A, Spitzer C, Singer GM, Graeber MB, Kreutzberg GW, Schwaiger FW (2001) Neuronal MCP-1 expression in response to remote nerve injury. J Cereb Blood Flow Metab 21:69-76.

Freter RR, Alberta JA, Lam KK, Stiles CD (1995) A new platelet-derived growth factor-regulated genomic element which binds a serine/threonine phosphoprotein mediates induction of the slow immediate-early gene MCP-1. Mol Cell Biol 15:315-325.

Gaboreanu A-M, Hrstka R, Xu W, Shy M, Kamholz J, Lilien J, Balsamo J (2007) Myelin protein zero/P0 phosphorylation and function require an adaptor protein linking it to RACK1 and PKC{alpha}. The Journal of Cell Biology 177:707-716.

Geissmann F, Jung S, Littman DR (2003) Blood monocytes consist of two principal subsets with distinct migratory properties. Immunity 19:71-82.

Gerits N, Kostenko S, Moens U (2007) In vivo functions of mitogen-activated protein kinases: conclusions from knock-in and knock-out mice. Transgenic Res 16:281-314.

Giese KP, Martini R, Lemke G, Soriano P, Schachner M (1992) Mouse P0 gene disruption leads to hypomyelination, abnormal expression of recognition molecules, and degeneration of myelin and axons. Cell 71:565-576.

Goebeler M, Gillitzer R, Kilian K, Utzel K, Brocker EB, Rapp UR, Ludwig S (2001) Multiple signaling pathways regulate NF-kappaB-dependent transcription of the monocyte chemoattractant protein-1 gene in primary endothelial cells. Blood 97:46-55.

Gonzalez-Amaro R, Sanchez-Madrid F (2002) [Intercellular adhesion molecules and chemotaxic factors in the pathogenesis of multiple sclerosis]. Rev Neurol 35:985-993.

Gordon S, Taylor PR (2005) Monocyte and macrophage heterogeneity. Nat Rev Immunol 5:953-964.

Guenard V, Montag D, Schachner M, Martini R (1996) Onion bulb cells in mice deficient for myelin genes share molecular properties with immature, differentiated non-myelinating, and denervated Schwann cells. Glia 18:27-38.

Hahn AF, Brown WF, Koopman WJ, Feasby TE (1990) X-linked dominant hereditary motor and sensory neuropathy. Brain 113 (Pt 5):1511-1525.

Harrisingh MC, Lloyd AC (2004) Ras/Raf/ERK signalling and NF1. Cell Cycle 3:1255-1258.

Harrisingh MC, Perez-Nadales E, Parkinson DB, Malcolm DS, Mudge AW, Lloyd AC (2004) The Ras/Raf/ERK signalling pathway drives Schwann cell dedifferentiation. Embo J 23:3061-3071.

Hayashi M, Luo Y, Laning J, Strieter RM, Dorf ME (1995) Production and function of monocyte chemoattractant protein-1 and other beta-chemokines in murine glial cells. J Neuroimmunol 60:143-150.

Huang DR, Wang J, Kivisakk P, Rollins BJ, Ransohoff RM (2001) Absence of monocyte chemoattractant protein 1 in mice leads to decreased local macrophage recruitment and antigen-specific T helper cell type 1 immune response in experimental autoimmune encephalomyelitis. J Exp Med 193:713-726.

Huxley C, Passage E, Manson A, Putzu G, Figarella-Branger D, Pellissier JF, Fontes M (1996) Construction of a mouse model of Charcot-Marie-Tooth disease type 1A by pronuclear injection of human YAC DNA. Hum Mol Genet 5:563-569.

Huxley C, Passage E, Robertson AM, Youl B, Huston S, Manson A, Saberan-Djoniedi D, Figarella-Branger D, Pellissier JF, Thomas PK, Fontes M (1998) Correlation between varying levels of PMP22 expression and the degree of demyelination and reduction in nerve conduction velocity in transgenic mice. Hum Mol Genet 7:449-458.

Ip CW, Kroner A, Fischer S, Berghoff M, Kobsar I, Maurer M, Martini R (2006) Role of immune cells in animal models for inherited peripheral neuropathies. Neuromolecular Med 8:175-190.

Ip WK, Wong CK, Lam CWK (2006) Interleukin (IL)-4 and IL-13 up-regulate monocyte chemoattractant protein-1 expression in human bronchial epithelial cells: involvement of p38 mitogen-activated protein kinase, extracellular signal-regulated kinase 1/2 and Janus kinase-2 but not c-Jun NH2-terminal kinase 1/2 signalling pathways. Clinical and Experimental Immunology 145:162-172.

Jessen KR, Brennan A, Morgan L, Mirsky R, Kent A, Hashimoto Y, Gavrilovic J (1994) The Schwann cell precursor and its fate: a study of cell death and differentiation during gliogenesis in rat embryonic nerves. Neuron 12:509-527.

Jessen KR, Mirsky R (2005) The origin and development of glial cells in peripheral nerves. Nat Rev Neurosci 6:671-682.

Johanson SO, Crouch MF, Hendry IA (1995) Retrograde axonal transport of signal transduction proteins in rat sciatic nerve. Brain Res 690:55-63.

Joseph Sambrook DR (2001) Molecular Cloning: A Laboratory Manual. Melbourne, Australia, Dallas, USA: Cold Spring Harbor Laboratory Press.

Karanth S, Yang G, Yeh J, Richardson PM (2006) Nature of signals that initiate the immune response during Wallerian degeneration of peripheral nerves. Exp Neurol 202:161-166.

Kobsar I, Maurer M, Ott T, Martini R (2002) Macrophage-related demyelination in peripheral nerves of mice deficient in the gap junction protein connexin 32. Neurosci Lett 320:17-20.

Kobsar I, Berghoff M, Samsam M, Wessig C, Maurer M, Toyka KV, Martini R (2003) Preserved myelin integrity and reduced axonopathy in connexin32-deficient mice lacking the recombination activating gene-1. Brain 126:804-813.

Kobsar I, Hasenpusch-Theil K, Wessig C, Muller HW, Martini R (2005) Evidence for macrophage-mediated myelin disruption in an animal model for Charcot-Marie-Tooth neuropathy type 1A. J Neurosci Res 81:857-864.

Kobsar I, Oetke C, Kroner A, Wessig C, Crocker P, Martini R (2006) Attenuated demyelination in the absence of the macrophage-restricted adhesion molecule sialoadhesin (Siglec-1) in mice heterozygously deficient in P0. Mol Cell Neurosci 31:685-691.

Koch A, Giembycz M, Ito K, Lim S, Jazrawi E, Barnes PJ, Adcock I, Erdmann E, Chung KF (2004) Mitogen-activated protein kinase modulation of nuclear factor-kappaB-induced granulocyte macrophage-colony-stimulating factor release from human alveolar macrophages. Am J Respir Cell Mol Biol 30:342-349.

Kramer BW, Gotz R, Rapp UR (2004) Use of mitogenic cascade blockers for treatment of C-Raf induced lung adenoma in vivo: CI-1040 strongly reduces growth and improves lung structure. BMC Cancer 4:24.

Laemmli UK (1970) Cleavage of structural proteins during the assembly of the head of bacteriophage T4. Nature 227:680-685.

Lindberg RL, Martini R, Baumgartner M, Erne B, Borg J, Zielasek J, Ricker K, Steck A, Toyka KV, Meyer UA (1999) Motor neuropathy in porphobilinogen deaminase-deficient mice imitates the peripheral neuropathy of human acute porphyria. J Clin Invest 103:1127-1134.

Loetscher P, Seitz M, Clark-Lewis I, Baggiolini M, Moser B (1996) Activation of NK cells by CC chemokines. Chemotaxis, Ca2+ mobilization, and enzyme release. J Immunol 156:322-327.

Loring JF, Erickson CA (1987) Neural crest cell migratory pathways in the trunk of the chick embryo. Dev Biol 121:220-236.

Lowry OH, Rosebrough NJ, Farr AL, Randall RJ (1951) Protein measurement with the Folin phenol reagent. J Biol Chem 193:265-275.

Lu B, Rutledge BJ, Gu L, Fiorillo J, Lukacs NW, Kunkel SL, North R, Gerard C, Rollins BJ (1998) Abnormalities in monocyte recruitment and cytokine expression in monocyte chemoattractant protein 1-deficient mice. J Exp Med 187:601-608.

Ludwin SK, Maitland M (1984) Long-term remyelination fails to reconstitute normal thickness of central myelin sheaths. J Neurol Sci 64:193-198.

Martin T, Cardarelli PM, Parry GC, Felts KA, Cobb RR (1997) Cytokine induction of monocyte chemoattractant protein-1 gene expression in human endothelial cells depends on the cooperative action of NF-kappa B and AP-1. Eur J Immunol 27:1091-1097.

Martinez FO, Sica A, Mantovani A, Locati M (2008) Macrophage activation and polarization. Front Biosci 13:453-461.

Martini R, Zielasek J, Toyka KV, Giese KP, Schachner M (1995a) Protein zero (P0)-deficient mice show myelin degeneration in peripheral nerves characteristic of inherited human neuropathies. Nat Genet 11:281-286.

Martini R, Mohajeri MH, Kasper S, Giese KP, Schachner M (1995b) Mice doubly deficient in the genes for P0 and myelin basic protein show that both proteins contribute to the formation of the major dense line in peripheral nerve myelin. J Neurosci 15:4488-4495.

Martini R (1997) Animal models for inherited peripheral neuropathies. Journal of Anatomy 191:321-336.

Martini R (2004) Schwann cells and Myelin. In: Neuroglia (Kettenmann H, Ransom, BR, ed): Oxford University Press.

Matsushima K, Larsen CG, DuBois GC, Oppenheim JJ (1989) Purification and characterization of a novel monocyte chemotactic and activating factor produced by a human myelomonocytic cell line. J Exp Med 169:1485-1490.

Maurer M, Muller M, Kobsar I, Leonhard C, Martini R, Kiefer R (2003) Origin of pathogenic macrophages and endoneurial fibroblast-like cells in an animal model of inherited neuropathy. Mol Cell Neurosci 23:351-359.

Meier C, Parmantier E, Brennan A, Mirsky R, Jessen KR (1999) Developing Schwann cells acquire the ability to survive without axons by establishing an autocrine circuit involving insulin-like growth factor, neurotrophin-3, and platelet-derived growth factor-BB. J Neurosci 19:3847-3859.

Middlemas A, Delcroix JD, Sayers NM, Tomlinson DR, Fernyhough P (2003) Enhanced activation of axonally transported stress-activated protein kinases in peripheral nerve in diabetic neuropathy is prevented by neurotrophin-3. Brain 126:1671-1682.

Mombaerts P, Iacomini J, Johnson RS, Herrup K, Tonegawa S, Papaioannou VE (1992) RAG-1-deficient mice have no mature B and T lymphocytes. Cell 68:869-877.

Morris JK, Lin W, Hauser C, Marchuk Y, Getman D, Lee KF (1999) Rescue of the cardiac defect in ErbB2 mutant mice reveals essential roles of ErbB2 in peripheral nervous system development. Neuron 23:273-283.

Muller M, Berghoff M, Kobsar I, Kiefer R, Martini R (2007) Macrophage colony stimulating factor is a crucial factor for the intrinsic macrophage response in mice heterozygously deficient for the myelin protein P0. Exp Neurol 203:55-62.

Naba I, Yoshikawa H, Sakoda S, Itabe H, Suzuki H, Kodama T, Yanagihara T (2000) Onion-bulb formation after a single compression injury in the macrophage scavenger receptor knockout mice. Exp Neurol 166:83-89.

Neote K, DiGregorio D, Mak JY, Horuk R, Schall TJ (1993) Molecular cloning, functional expression, and signaling characteristics of a C-C chemokine receptor. Cell 72:415-425.

Niemann A, Berger P, Suter U (2006) Pathomechanisms of mutant proteins in Charcot-Marie-Tooth disease. Neuromolecular Med 8:217-242.

Nodari A, Zambroni D, Quattrini A, Court FA, D'Urso A, Recchia A, Tybulewicz VL, Wrabetz L, Feltri ML (2007) Beta1 integrin activates Rac1 in Schwann cells to generate radial lamellae during axonal sorting and myelination. J Cell Biol 177:1063-1075.

Ogata T, Iijima S, Hoshikawa S, Miura T, Yamamoto S, Oda H, Nakamura K, Tanaka S (2004) Opposing extracellular signal-regulated kinase and Akt pathways control Schwann cell myelination. J Neurosci 24:6724-6732.

Okabe M, Ikawa M, Kominami K, Nakanishi T, Nishimune Y (1997) 'Green mice' as a source of ubiquitous green cells. FEBS Lett 407:313-319.

Paul DL (1995) New functions for gap junctions. Curr Opin Cell Biol 7:665-672.

Perrin FE, Lacroix S, Aviles-Trigueros M, David S (2005) Involvement of monocyte chemoattractant protein-1, macrophage inflammatory protein-1alpha and interleukin-1beta in Wallerian degeneration. Brain 128:854-866.

Ping D, Jones PL, Boss JM (1996) TNF regulates the in vivo occupancy of both distal and proximal regulatory regions of the MCP-1/JE gene. Immunity 4:455-469.

Ping D, Boekhoudt G, Boss JM (1999a) trans-Retinoic acid blocks platelet-derived growth factor-BB-induced expression of the murine monocyte chemoattractant-1 gene by blocking the assembly of a promoter proximal Sp1 binding site. J Biol Chem 274:31909-31916.

Ping D, Boekhoudt GH, Rogers EM, Boss JM (1999b) Nuclear factor-kappa B p65 mediates the assembly and activation of the TNF-responsive element of the murine monocyte chemoattractant-1 gene. J Immunol 162:727-734.

Ping D, Boekhoudt G, Zhang F, Morris A, Philipsen S, Warren ST, Boss JM (2000) Sp1 binding is critical for promoter assembly and activation of the MCP-1 gene by tumor necrosis factor. J Biol Chem 275:1708-1714.

Pixley FJ, Stanley ER (2004) CSF-1 regulation of the wandering macrophage: complexity in action. Trends Cell Biol 14:628-638.

Poliak S, Peles E (2003) The local differentiation of myelinated axons at nodes of Ranvier. Nat Rev Neurosci 4:968-980.

Riethmacher D, Sonnenberg-Riethmacher E, Brinkmann V, Yamaai T, Lewin GR, Birchmeier C (1997) Severe neuropathies in mice with targeted mutations in the ErbB3 receptor. Nature 389:725-730.

Rollins BJ, Morrison ED, Stiles CD (1988) Cloning and expression of JE, a gene inducible by platelet-derived growth factor and whose product has cytokine-like properties. Proc Natl Acad Sci U S A 85:3738-3742.

Roux PP, Blenis J (2004) ERK and p38 MAPK-activated protein kinases: a family of protein kinases with diverse biological functions. Microbiol Mol Biol Rev 68:320-344.

Sanders SK, Crean SM, Boxer PA, Kellner D, LaRosa GJ, Hunt SW, 3rd (2000) Functional differences between monocyte chemotactic protein-1 receptor A and monocyte chemotactic protein-1 receptor B expressed in a Jurkat T cell. J Immunol 165:4877-4883.

Scherer SS, Salzer JL (1996) Axon-Schwann cell interaction during peripheral nerve degeneration and regeneration. In: Glial cell development, 1st Edition (Jessen KR, Richardson WD, ed), pp 165-196. Oxford: Bios Scientific Publishers Ltd.

Schilling M, Besselmann M, Muller M, Strecker JK, Ringelstein EB, Kiefer R (2005) Predominant phagocytic activity of resident microglia over hematogenous macrophages following transient focal cerebral ischemia: an investigation using green fluorescent protein transgenic bone marrow chimeric mice. Exp Neurol 196:290-297.

Schlueter AJ, Glasgow JK (2006) Phenotypic comparison of multiple monocyte-related populations in murine peripheral blood and bone marrow. Cytometry A 69:281-290.

Schmid CD, Stienekemeier M, Oehen S, Bootz F, Zielasek J, Gold R, Toyka KV, Schachner M, Martini R (2000) Immune deficiency in mouse models for inherited peripheral neuropathies leads to improved myelin maintenance. Journal of Neuroscience 20:729-735.

Sebolt-Leopold JS, Dudley DT, Herrera R, Van Becelaere K, Wiland A, Gowan RC, Tecle H, Barrett SD, Bridges A, Przybranowski S, Leopold WR, Saltiel AR (1999) Blockade of the MAP kinase pathway suppresses growth of colon tumors in vivo. Nat Med 5:810-816.

Sebolt-Leopold JS (2000) Development of anticancer drugs targeting the MAP kinase pathway. Oncogene 19:6594-6599.

Serbina NV, Pamer EG (2006) Monocyte emigration from bone marrow during bacterial infection requires signals mediated by chemokine receptor CCR2. Nat Immunol 7:311-317.

Serbina NV, Jia T, Hohl TM, Pamer EG (2008) Monocyte-mediated defense against microbial pathogens. Annu Rev Immunol 26:421-452.

Sereda M, Griffiths I, Puhlhofer A, Stewart H, Rossner MJ, Zimmerman F, Magyar JP, Schneider A, Hund E, Meinck HM, Suter U, Nave KA (1996) A transgenic rat model of Charcot-Marie-Tooth disease. Neuron 16:1049-1060.

Sharma K, Korade Z, Frank E (1995) Late-migrating neuroepithelial cells from the spinal cord differentiate into sensory ganglion cells and melanocytes. Neuron 14:143-152.

Sheng WS, Hu S, Ni HT, Rowen TN, Lokensgard JR, Peterson PK (2005) TNF-alpha-induced chemokine production and apoptosis in human neural precursor cells. J Leukoc Biol 78:1233-1241.

Shy ME, Garbern JY, Kamholz J (2002) Hereditary motor and sensory neuropathies: a biological perspective. Lancet Neurol 1:110-118.

Shy ME (2006) Peripheral neuropathies caused by mutations in the myelin protein zero. J Neurol Sci 242:55-66.

Sica A, Wang JM, Colotta F, Dejana E, Mantovani A, Oppenheim JJ, Larsen CG, Zachariae CO, Matsushima K (1990) Monocyte chemotactic and activating factor gene expression induced in endothelial cells by IL-1 and tumor necrosis factor. J Immunol 144:3034-3038.

Skre H (1974) Genetic and clinical aspects of Charcot-Marie-Tooth's disease. Clin Genet 6:98-118.

Stoll G, Jander S, Myers RR (2002) Degeneration and regeneration of the peripheral nervous system: from Augustus Waller's observations to neuroinflammation. J Peripher Nerv Syst 7:13-27.

Sunderkotter C, Nikolic T, Dillon MJ, Van Rooijen N, Stehling M, Drevets DA, Leenen PJ (2004) Subpopulations of mouse blood monocytes differ in maturation stage and inflammatory response. J Immunol 172:4410-4417.

Suter U, Snipes GJ (1995) Biology and genetics of hereditary motor and sensory neuropathies. Annu Rev Neurosci 18:45-75.

Suter U, Scherer SS (2003) Disease mechanisms in inherited neuropathies. Nat Rev Neurosci 4:714-726.

Swank MW, Sweatt JD (2001) Increased histone acetyltransferase and lysine acetyltransferase activity and biphasic activation of the ERK/RSK cascade in insular cortex during novel taste learning. J Neurosci 21:3383-3391.

Takeshita A, Chen Y, Watanabe A, Kitano S, Hanazawa S (1995) TGF-beta induces expression of monocyte chemoattractant JE/monocyte chemoattractant protein 1 via transcriptional factor AP-1 induced by protein kinase in osteoblastic cells. J Immunol 155:419-426.

Tanaka T, Minami M, Nakagawa T, Satoh M (2004) Enhanced production of monocyte chemoattractant protein-1 in the dorsal root ganglia in a rat model of neuropathic pain: possible involvement in the development of neuropathic pain. Neurosci Res 48:463-469.

Taskinen HS, Roytta M (2000) Increased expression of chemokines (MCP-1, MIP-1alpha, RANTES) after peripheral nerve transection. J Peripher Nerv Syst 5:75-81.

Toews AD, Barrett C, Morell P (1998) Monocyte chemoattractant protein 1 is responsible for macrophage recruitment following injury to sciatic nerve. J Neurosci Res 53:260-267.

Tofaris GK, Patterson PH, Jessen KR, Mirsky R (2002) Denervated Schwann cells attract macrophages by secretion of leukemia inhibitory factor (LIF) and monocyte chemoattractant protein-1 in a process regulated by interleukin-6 and LIF. J Neurosci 22:6696-6703.

Trapp B, Kidd, GJ (2004) Structure of the Myelinated Axon. In: Myelin Biology and Disorder (Lazzarini R, ed). London: Elsevier Academic Press.

Ueda A, Okuda K, Ohno S, Shirai A, Igarashi T, Matsunaga K, Fukushima J, Kawamoto S, Ishigatsubo Y, Okubo T (1994) NF-kappa B and Sp1 regulate transcription of the human monocyte chemoattractant protein-1 gene. J Immunol 153:2052-2063.

Valente AJ, Graves DT, Vialle-Valentin CE, Delgado R, Schwartz CJ (1988) Purification of a monocyte chemotactic factor secreted by nonhuman primate vascular cells in culture. Biochemistry 27:4162-4168.

Van Damme J, Proost P, Lenaerts JP, Opdenakker G (1992) Structural and functional identification of two human, tumor-derived monocyte chemotactic proteins (MCP-2 and MCP-3) belonging to the chemokine family. J Exp Med 176:59-65.

Vargas ME, Barres BA (2007) Why is Wallerian degeneration in the CNS so slow? Annu Rev Neurosci 30:153-179.

Vass K, Hickey W, Schmidt R, Lassmann H (1993) Bone marrow-derived elements in the peripheral nervous system. An immunohistochemical and ultrastructural investigation in chimeric rats. Lab Invest 69:275-282.

Venkatesan BA, Mahimainathan L, Ghosh-Choudhury N, Gorin Y, Bhandari B, Valente AJ, Abboud HE, Choudhury GG (2006) PI 3 kinase-dependent Akt kinase and PKCepsilon independently regulate interferon-gamma-induced STAT1alpha serine

phosphorylation to induce monocyte chemotactic protein-1 expression. Cell Signal 18:508-518.

Visan L (2003) P0 specific T-cell repertoire in wild-type and P0 deficient mice. In: Neurologische Klinik und Poliklinik. Würzburg: Julius-Maximillians-Universität Würzburg.

Waetzig V, Czeloth K, Hidding U, Mielke K, Kanzow M, Brecht S, Goetz M, Lucius R, Herdegen T, Hanisch UK (2005) c-Jun N-terminal kinases (JNKs) mediate pro-inflammatory actions of microglia. Glia 50:235-246.

Wallquist W, Plantman S, Thams S, Thyboll J, Kortesmaa J, Lannergren J, Domogatskaya A, Ogren SO, Risling M, Hammarberg H, Tryggvason K, Cullheim S (2005) Impeded interaction between Schwann cells and axons in the absence of laminin alpha4. J Neurosci 25:3692-3700.

Wanner IB, Guerra NK, Mahoney J, Kumar A, Wood PM, Mirsky R, Jessen KR (2006) Role of N-cadherin in Schwann cell precursors of growing nerves. Glia 54:439-459.

Woldeyesus MT, Britsch S, Riethmacher D, Xu L, Sonnenberg-Riethmacher E, Abou-Rebyeh F, Harvey R, Caroni P, Birchmeier C (1999) Peripheral nervous system defects in erbB2 mutants following genetic rescue of heart development. Genes and Development 13:2538-2548.

Xu W, Shy M, Kamholz J, Elferink L, Xu G, Lilien J, Balsamo J (2001) Mutations in the cytoplasmic domain of P0 reveal a role for PKC-mediated phosphorylation in adhesion and myelination. J Cell Biol 155:439-446.

Yoo JK, Kwon H, Khil L-Y, Zhang L, Jun H-S, Yoon J-W (2005) IL-18 induces monocyte chemotactic protein-1 production in macrophages through the phosphatidylinositol 3-kinase/Akt and MEK/ERK1/2 pathways. J Immunol 175:8280-8286.

Yoshida H, Hayashi S, Kunisada T, Ogawa M, Nishikawa S, Okamura H, Sudo T, Shultz LD, Nishikawa S (1990) The murine mutation osteopetrosis is in the coding region of the macrophage colony stimulating factor gene. Nature 345:442-444.

Yoshimura T, Yuhki N, Moore SK, Appella E, Lerman MI, Leonard EJ (1989a) Human monocyte chemoattractant protein-1 (MCP-1). Full-length cDNA cloning, expression in mitogen-stimulated blood mononuclear leukocytes, and sequence similarity to mouse competence gene JE. FEBS Lett 244:487-493.

Yoshimura T, Robinson EA, Tanaka S, Appella E, Kuratsu J, Leonard EJ (1989b) Purification and amino acid analysis of two human glioma-derived monocyte chemoattractants. J Exp Med 169:1449-1459.

Yoshimura H, Nakahama K, Safronova O, Tanaka N, Muneta T, Morita I (2006) Transforming growth factor-beta stimulates IL-1beta-induced monocyte chemoattractant protein-1 expression in human synovial cells via the ERK/AP-1 pathway. Inflamm Res 55:543-549.

Zhang J, De Koninck Y (2006) Spatial and temporal relationship between monocyte chemoattractant protein-1 expression and spinal glial activation following peripheral nerve injury. J Neurochem 97:772-783.

9. Abbreviations

AKT	Protein kinase B
BSA	Bovine serum albumine
CCL	Chemokine (C-C motif) ligand
CCR	Chemokine (C-C motif) receptor
CD	Cluster of differentiation
Cdc	Cell division control protein
cDNA	Complementary DNA
CMT	Charcot-Marie-Tooth disease
Cx	Connexin
DEPC	Diethylpyrocarbonate
DMEM	Dulbecco`s modified eagle medium
DMSO	Dimethyl sulfoxide
DNA	Deoxyribonucleic acid
dNTP	Deoxynucelosidtriphosphate
DSS	Dejerine-Sottas syndrome
EAE	Experimental autoimmune encephalomyelitis
EDTA	Ethylene diamine tetraacetic acid
ELISA	Enzyme-linked immunosorbent assay
ERK	Extracellular-signal regulated kinase
FCS	Foetal calf serum
GFAP	Glial fibrillary acidic protein
GFP	Green fluorescent protein
GjB	Gap junction protein, beta 1
GM-CSF	Granulocyte-macrophage colony stimulating factor
GTP	Guanosine triphosphate
HNPP	Hereditary neuropathies with liability to pressure palsies
IFNγ	Interferon γ
IGF	Insulin-like growth factor
IκBα	Nuclear factor of kappa light polypeptide gene enhancer in B-cells inhibitor, alpha
IL	Interleukin
JNK	C-Jun N-terminal kinases
LIF	Leukemia inhibitory factor
MAG	Myelin associated glycoprotein

MAPK	Mitogen-activated protein kinase
MCP-1	Monocyte chemoattractant protein
M-CSF	Macrophage colony stimulating factor
MEK	MAPK-ERK-kinase
MPZ	Myelin protein zero
NFκB	Nuclear factor of kappa light polypeptide gene enhancer in B-cells
NGF	Nerve growth facto
NT	Neurotrohpin
OCT6	octamer-binding transcription factor
P0	Myelin protein zero
PBS	Phosphate buffered saline
PCR	Polymerase chain reaction
PDGF	Platelet derived growth factor
PFA	Paraformaldehyde
phosphoERK1/2	phosphorylated ERK1/2
PI3K	Phosphoinositol-3-kinase
PKC	Protein kinase C
PLP	Proteolipid protein
PMP22	Peripheral myelin protein 22
qRT-PCR	semiquantitative real-time PCR
RAG	Recombination activating gene
RNA	Ribonucleosid acid
rRNA	ribosomal RNA
S100β	S100 calcium binding protein β
SD	Standard deviation
SDS	Sodium dodecylsulfate
SDS-PAGE	SDS Polyacrylamide gel electrophoresis
SIMPLE	LPS-induced TN-factor
STAT	Signal transducers and activator of transcription
TBE	Tris-borate-EDTA
TCR	T-cell receptor
TGF	Transforming growth factor
Th2	T-helper type 2
TNFα	Tumor necrosis factor
Trk	neurotrophic tyrosine kinase receptor
U	Unit [µmol/min]

10. Danksagung

Mein besonderer Dank gilt Prof. Dr. Rudolf Martini für die wissenschaftlich und menschlich ausgewogene Betreuung, für die finanzielle Grundlage, für den unermesslichen Schatz an Wissen, für die Bereitschaft immer wieder Neues zu testen und zu diskutieren, für die Geduld und insbesondere für die Freiheit beim Erstellen dieser Arbeit. Ohne diese harmonischen und idealen Bedingungen wäre die Arbeit nicht in dieser Form möglich gewesen.

Herrn Prof. Dr. Jakob Troppmair möchte ich danken für seine Kenntnisse und Unterstützung, sowie sein persönliches Engagement, womit die Untersuchungen der Signaltransduktion erst möglich wurden.

Herrn Prof. Dr. Thomas Hünig danke ich für die Möglichkeiten, Diskussionen und Anregungen in hervorragender Atmosphäre, die mir im Rahmen des Graduiertenkollegs „Immunmodulation“ zuteil wurden.

Herrn Prof. Dr. Klaus V. Toyka möchte ich besonders danken für angeregte Diskussionen, als auch für den wissenschaftlichen und musikalischen Rahmen.

Meinen Kollegen und Freunden, die ich im Rahmen des Graduiertenkollegs und am Institut fand, möchte ich danken für die stete Hilfe im Alltag, aber insbesondere für Geduld, Hilfsbereitschaft, Toleranz und Selbstironie. Insbesondere möchte ich mich bei Heinrich Blazyca, Caroline Kiesel, Astrid Drasche und Nadine Weckesser für Ihren Beitrag bedanken. Besonderer Dank gebührt Helga Brünner und Karl-Heinz Aulenbach für die Organisation und Pflege der Tiere.

Meiner Großmutter Elfriede Kaiser und meiner Mutter Gabriele Fischer danke ich für alles, was sie mir mit auf den Weg gegeben haben und die Zeit die wir miteinander verbrachten.

Besonderer Dank gilt allen in meiner Familie oder aus meinem Bekannten- und Freundeskreis, die mir während dieser Zeit Unterstützung gaben oder mich daran erinnerten, was mir Wert ist.

Herzlichen Dank, Caroline!

11. Curriculum vitae

Persönliche Daten

Name:	Stefan Martin Fischer
Gerbutstag und -ort:	30.05.1977 in Bamberg
Familienstand:	ledig
Eltern:	Gabriele Fischer (*04.01.1948, + 31.03.2008) Johann Hacker (*22.09.1928)

Berufliche Tätigkeit

seit 04/2006	Wissenschaftlicher Mitarbeiter, Neurologische Klinik und Poliklinik, Experimentelle Entwicklungsneurobiologie, Prof. Dr. Rudolf Martini, Julius-Maximilians-Universität, Würzburg
04/2003 – 03/2006	Stipendiat der Deutschen Forschungsgemeinschaft im Rahmen des Graduiertenkollegs “Immunmodulation”, Prof. Dr. Thomas Hünig, Julius-Maximilians-Universität, Würzburg
10/1996 – 03/1997	Angestellter der Deutschen Telekom AG, Bamberg

Hochschulstudium

02/2003	Diplomarbeit in der Abteilung für Biotechnologie, Institut für Biochemie und Biologie, Universität Potsdam Titel: „Oligomere bispezifische Antikörper”
10/1997 – 03/2003	Studium der Biochemie (Diplom), Universität Potsdam

Schulbildung

06/1996	Allgemeine Hochschulreife; Dientzenhofer Gymnasium, Bamberg
09/1987 – 06/1996	Dientzenhofer Gymnasium, Bamberg
09/1983 – 08/1987	Luitpoldschule, Bamberg

12. Publications

Original article:

Ip CW, Kroner A, Bendszus M, Leder C, Kobsar I, **Fischer S**, Wiendl H, Nave KA, Martini R. J Neurosci. 2006; 2;26(31):8206-16.
"Immune cells contribute to myelin degeneration and axonopathic changes in mice overexpressing proteolipid protein in oligodendrocytes"

Fischer S, Kleinschnitz C, Müller M, Kobsar I, Ip CW, Rollins B, Martini R. Mol Cell Neurosci. 2008; 37(2):359-66.
"Monocyte chemoattractant protein-1 is a pathogenic component in a model for a hereditary peripheral neuropathy"

Fischer S, Weishaupt A, Troppmair J, Martini R. Glia 2008, 56(8):836-843.
"Increase of MCP-1 (CCL2) in myelin mutant Schwann cells is mediated by MEK-ERK signaling pathway"

Review article:

Ip CW, Kroner A, **Fischer S**, Berghoff M, Kobsar I, Mäurer M, Martini R. NeuroMolecular Medicine, 2006, 8 (1-2):175-90
"Role of immune cells in animal models for peripheral neuropathies"

Martini R, **Fischer S**, López-Vales R, David S. Glia, *submitted*
Interactions between Schwann cells and macrophages in injury and inherited demyelinating disease

Oral presentation:

Fischer S et al., 2005, Oral presentation, Peripheral Nerve Society Biennial Meeting, Tuscany, Italy
"P0 +/- Mice Show Increased ERK-Phosphorylation And MCP-1 Expression At Initial Stages Of Genetically-Mediated Demyelination"

Fischer S et al., 2005, Poster presentation, Gesellschaft für Biochemie und Molekularbiologie (GBM) Annual Fall meeting, Berlin/Potsdam

"Mice deficient for the Myelin component P0 show increased ERK-phosphorylation and MCP-1 expression at initial stages of primarily genetically-mediated demyelination"

13. Eidesstattliche Erklärung

Hiermit erkläre ich, die vorliegende Arbeit selbständig angefertigt und keine anderen als die angegebenen Hilfsmittel verwendet zu haben.
Diese Arbeit hat weder in gleicher noch in ähnlicher Form in einem anderen Prüfungsverfahren vorgelegen.
Ich habe in keinem früheren Verfahren einen akademischen Grad erworben oder zu erwerben versucht.

Würzburg, 14.07.08

_____

Stefan Fischer